

# **LOW ALTITUDE DRONE ASSISTED DETECTION OF METEORITES IN THE AUSTRALIAN DESERT**

Adrian Johnathon Orellana

Bachelor of Engineering  
Mechatronic Engineering Major

This is a very good thesis that shows significant progress. Adrian has demonstrated significant independence and insight in this work, and has produced a sensor suite that will likely see further use. It doesn't look well polished, with many missing figure references, and many figures with weak captions and missing legends. Ultimately it would have been nice to see some data analysis from the full sensor suite, but Adrian has nevertheless accomplished a great deal.



Department of Electronic Engineering  
Macquarie University

November 15, 2016

Supervisor: Dr. David Inglis

Copyright © 2016 Adrian Johnathon Orellana

All Rights Reserved

MACQUARIE UNIVERSITY

DEPARTMENT APPROVAL

of a senior thesis submitted by

Adrian Johnathon Orellana

This thesis has been reviewed by the research advisor, research coordinator, and department chair and has been found to be satisfactory.

---

Date

---

Supervisor: Dr. David Inglis, Advisor

---

Date

---

A, Research Coordinator

---

Date

---

B, Chair

## **STATEMENT OF CANDIDATE**

I, Adrian Orellana submit this report as part of the requirement for the award of a Bachelor of Engineering in the Department of Electronic Engineering, Macquarie University. I declare that the ideas, designs and experimental work, results, analyses and conclusions set out in this dissertation are entirely my own effort. unless otherwise referenced or acknowledged. I further certify that the work is original and has not been previously submitted for qualification or assessment in any other course or academic institution.

Student's Name: Adrian J. Orellana

Student's Signature:

A handwritten signature in black ink, appearing to read "Adrian J. Orellana".

Date:

## **ACKNOWLEDGMENTS**

Foremost, I would like to thank my supervisor Dr. David Inglis for his guidance and understanding, not only through his feedback and contribution to this research project but also for his continued support throughout my university career. His support of my research and advice on academic writing and thesis structure has been invaluable. I would also like to thank Dr. Craig O'Neill for contributing not only his knowledge and interest in meteorites and geology, but for his valuable contributions in the form of loaning parts of the hardware that made building the system possible as well as the providing of multiple meteorites for testing purposes. In addition, would also like to acknowledge that without his initial proposal and interest this research project would not have commenced. Lastly, I would like to thank my colleague and peer Ryan Barnes for providing technical advice on the project as well as providing access to his 3D printing resources.

## ABSTRACT

The detection and identification of Australian meteorites is a task of great scientific interest and due to meteorites being the only significant source of material from other planets and asteroids, are of immense scientific value. New meteorites have the potential to stimulate new research and ideas in cosmo-chemistry, planetary geology, astronomy, and astrobiology.

Currently the most effective method for the detection of meteorites is by eye, or with handheld magnetic survey equipment, employed by teams of researchers spread out over an area of interest. These manned expeditions in remote areas can be dangerous and cost significant resources to support and maintain. The use of a drone, will mitigate much of the risk associated with these types of surveys and as such the basis of this research project is to investigate the feasibility of meteorite detection using a magnetic gradiometer sensor suite to be fitted to an Unmanned Aerial Vehicle (UAV).

The proposed approach would allow for a considerable increase in geographic coverage and reduction in human resources as well as giving significant productivity and cost gains over conventional airborne surveys. Drones are incredibly well suited for many areas of terrestrial exploration, they can be mobilized and launched with minimal effort and require only a small team to operate and maintain. This work has clear relevance in an incredibly diverse range of search applications, such as the discovery of unexploded ordnance (UXOs), archaeological sites and/or items, geological interests, and mineral deposits, to planetary exploration, weather prediction and medical monitoring.

A key component of this project was the design and construction of a magnetic sensor suite for deployment on a drone platform. A testing system was developed to analyse and interpret this data to determine the location of any objects of interest. The collection of magnetic data on various meteorites and terrestrial rocks was performed with combined magnetic sensors in laboratory and field tests.

An investigation into the feasibility of on-board filtering vs post-collection filtering was performed and it was found that with a sufficiently powerful microcontroller and a robust wireless communication system it is entirely plausible that a drone system could locate and log potential meteorite locations in real time. In addition to this, the sensor suite was configured to mitigate noise from the electrical components of any potential drone system however the magnetic sensing suite will require additional refinement to correctly support its use on an aerial vehicle.

The findings of this research project indicate that the use of magnetic sensing is an appropriate way to detect meteorites at low altitudes from a moving unmanned aerial vehicle. While the software which enables the meteorite detection system to perform the magnetic detection and signal processing has been developed, the hardware requires additional work. As such this research project also identifies that further work is needed to efficiently deploy the meteorite detection suite in the field.

would have been nice to come to some more concrete conclusions on the performance envelope. Or if you did, to put them in the abstract.



# Contents

<b>Acknowledgments</b>	<b>v</b>
<b>Abstract</b>	<b>vi</b>
<b>Table of Contents</b>	<b>ix</b>
<b>List of Figures</b>	<b>xiii</b>
<b>List of Tables</b>	<b>xvii</b>
<b>1 Introduction</b>	<b>1</b>
1.1 Motivation . . . . .	1
1.2 Project Overview . . . . .	2
1.3 Objectives . . . . .	2
1.3.1 Technical Objectives . . . . .	3
1.3.2 Design Objectives . . . . .	3
1.3.3 Research Objectives . . . . .	3
1.3.4 Tasks Outside the Scope of This Project . . . . .	4
<b>2 Literature Review</b>	<b>5</b>
2.1 Meteorites . . . . .	5
2.1.1 Justification . . . . .	5
2.1.2 Current Methods of Meteorite Detection . . . . .	5
2.1.3 Attempts at the Autonomous Detection of Meteorites . . . . .	6
2.2 The Viability of the Australian Landscape . . . . .	6
2.3 Magnetic Materials . . . . .	8
2.3.1 Understanding Magnetic Fields . . . . .	8
2.3.2 Magnetic Gradient . . . . .	9
2.3.3 Magnetic Sensors . . . . .	10
2.3.4 Magnetic Gradiometers . . . . .	13
2.3.5 Applications of Gradiometers . . . . .	13
2.4 Digital Signal Processing . . . . .	14
2.4.1 Digital and Analogue Filters . . . . .	14

<b>3 Project Methodology</b>	<b>15</b>
3.1 Methodology Introduction . . . . .	15
3.2 Project Considerations . . . . .	16
3.2.1 Sensor Suite . . . . .	16
3.2.2 Data . . . . .	16
3.2.3 Noise . . . . .	16
3.2.4 Preparation for UAV Deployment . . . . .	16
3.2.5 Materials . . . . .	17
3.2.6 Project Scope . . . . .	17
3.3 Resource Requirements . . . . .	18
3.3.1 Hardware . . . . .	18
3.4 Meteorite Testing Samples . . . . .	23
3.5 Sensor Test-Bed Development . . . . .	24
3.5.1 Simulation of Operating Conditions . . . . .	24
3.5.2 Mechanical Design . . . . .	25
3.5.3 Gradiometer Implementation . . . . .	26
3.6 Signal to Noise . . . . .	26
3.6.1 Digital Signal Processing . . . . .	28
3.7 Building the Labview Testing Environment and User Interface . . . . .	30
<b>4 Sensor Suite Development</b>	<b>31</b>
4.1 Operational Limitations of Fluxgate Magnetometers . . . . .	32
4.1.1 Determination of Ideal Sensor Height . . . . .	32
4.1.2 Determination of Ideal Flight Speeds . . . . .	33
4.2 Sensor Suite Noise . . . . .	34
4.2.1 Analogue Noise . . . . .	34
4.2.2 Noise Considerations . . . . .	34
4.2.3 Establishing Sensor Accuracy and Resolution . . . . .	35
4.2.4 Aliasing . . . . .	37
4.2.5 Digital Compensation for Analogue Noise . . . . .	39
4.3 Gradiometric Implementation of Fluxgate Magnetometers on the Sensor Suite . . . . .	42
4.3.1 Sensor Orientation and Tilt . . . . .	44
4.3.2 Influence on Aliasing . . . . .	47
4.3.3 Individual Fluxgate Sensors Vs Magnetic Gradient . . . . .	48
4.3.4 Prevalence of Noise in a Gradiometric Sensor . . . . .	50
4.4 Initial Design Prototyping . . . . .	51
4.4.1 CAD . . . . .	51
4.4.2 Materials and Parts List . . . . .	51
4.5 Final Prototype . . . . .	52
4.5.1 Sensor Orientation and Layout . . . . .	52
4.5.2 Sensor Suite CAD . . . . .	52
4.6 Production . . . . .	53

4.7	Data Imported for the Sensor Suite . . . . .	54
<b>5</b>	<b>Conclusion and Outlook</b>	<b>57</b>
<b>A</b>	<b>Sensor Test-Bed Code</b>	<b>59</b>
A.1	Teensy 3.2 Testing Code . . . . .	60
<b>B</b>	<b>name of appendix B</b>	<b>61</b>
<b>C</b>	<b>Final Design Documents</b>	<b>63</b>
C.1	Detailed Sensor Suite Designs . . . . .	63
	<b>Bibliography</b>	<b>66</b>
	<b>References</b>	<b>67</b>



# List of Figures

2.1	<i>Geographical distribution of meteorite finds and observed falls in Australia. While accurate at depicting the prevalence and locations of meteorite finds across Australia, due to the publish date of the data, (1996) there has been a considerable increase in the amount of finds across these regions.</i> . . . . .	7
2.2	<i>A magnetic field is a vector quantity with both magnitude and direction properties [13]</i> . . . . .	8
2.3	<i>An assortment of magnetic sensor technology and their respective sensing ranges [16]</i> . . . . .	10
2.4	<i>Magnetic Field Sensors are categorised into two distinct types based on their magnetic field strengths and their measurement ranges. With magnetometers measuring low fields and gaussmeters measuring high magnetic fields, magnetometers were the obvious choice for this research project.</i> . . . . .	11
2.5	<i>Operation of a Fluxgate Magnetometer Coil</i> . . . . .	12
3.1	<i>The Intended Design of the Sensor Suite from Research Conducted</i> . . . . .	17
3.2	<i>While the Teensy 3.2 still used the standard 0.1inch pin spacing for breadboarding, it also features SMD headers on the underside allowing for over 34 I/O Pins</i> . . . . .	18
3.3	<i>Consisting of 10 analogue inputs, 6 analogue outputs, audio channels, and 40 digital input/output (DIO) pins. The NI myRIO also includes an on-board WiFi module, a three-axis accelerometer, and several LEDs.</i> . . . . .	19
3.4	<i>The pin layout of the myRIO's MXP identical connectors A and B</i> . . . . .	20
3.5	<i>The design specifications of the FLC-100</i> . . . . .	20
3.6	<i>The design specifications of the FLC-370</i> . . . . .	21
3.7	<i>The design of the GPS smart antenna module, LS20031 [28]</i> . . . . .	22
3.8	<i>The Five Meteorites Donated by Craig O'Neill of the Department of Earth and Planetary Sciences</i> . . . . .	23
3.9	<i>The Initial Design Prototype of the Sensor Test-Bed</i> . . . . .	24
3.10	<i>The basic premise for establishing the feasibility of this research project</i> . .	25
3.11	<i>The initial test bed for a single FLC-100 sensor</i> . . . . .	26
3.12	<i>The standard implementation of a gradiometric setup for testing, this was fixed to the sensor mount seen in Figure 3.11 and was the method used for all gradiometric calculations</i> . . . . .	26

3.13 Example of a FLC-370 signal containing noise . . . . .	27
3.14 The graphical user interface that was built for the purpose of testing the system, while the implementation of this should not be used during the actual deployment of the sensor because of the load it would place on the myRIO, this interface was essential for testing purposes, and is identical to the 'bare-bones' program except no data is fed to the UI . . . . .	30
4.1 Flux Density $B$ as measured by a single FLC-100 sensor, the limiting factor of distance was a major concern that will need to be addressed . . . . .	32
4.2 This figure displays the various in signal compression as speed increases. We also see a reduction in the height of the waveform which results in a signal height equal to that of a noise peak. This can be best seen in d) at $5ms^1$ . . . . .	33
4.3 The accuracy of the FLC-100 when measuring the Earth's Magnetic Field, in order to ensure that noise was kept to a minimum, experiment was conducted at 10pm with a shielded cable and the FLC-100 a minimum of 80cm from any external circuitry. A simple temperature sensor gave the room temperature at $16^\circ C$ . . . . .	35
4.4 Bin Ranges of the variation when measuring the Earth's magnetic field . .	35
4.5 The accuracy of the FLC-370 when measuring the Earth's Magnetic Field with a Voltage input of 5V, the experiment was conducted at 9:30pm with a shielded cable and the FLC-370 a minimum of 80cm from any external circuitry. A simple temperature sensor gave the room temperature at $18^\circ C$ . . . . .	36
4.6 Bin Ranges of the variation when measuring the Earth's magnetic field . .	36
4.7 Here we can see the very real effects that aliasing has on data provided from the FLC-100 as the sampling rate is increased from 0.5kHz at half the bandwidth ( $1/2f_b$ ) to 1kHz( the sensor bandwidth $f_b$ ) . . . . .	37
4.8 Visually there is no aliasing at a sampling frequency of 250Hz . . . . .	37
4.9 The two waveforms from Figure 4.7 plotted in the Frequency Domain, note the occurrence of an 11Hz wave, this was assumed to be the result of the aliased waveform . . . . .	38
4.10 Three of a number of FFTs attempted to determine the frequency content of the noise signal. . . . .	39
4.11 This figure attempts to illustrate the results of the various experiments conducted to determine the effectiveness of these filter on a digital signal. As can be seen, for a 7-point moving average roughly two thirds of the noise is removed and with a 7-point quadratic function only about half the noise is removed . . . . .	40
4.12 The Effects of Moving Average Filters vs Savitzky-Golay for increasing values of $N$ . . . . .	41

4.13 This signal is filtered with increasing values of points $N$ . As the number of points increases the noise becomes significantly less defined, this can be seen in the S/N plot of the same data following, see Figure 4.14, however it is important to note that the edges also become less sharp. This may prove to be an issue for the sharp pulses that are produced when measuring a magnetic field at increased speeds . . . . .	42
4.14 The Signal to Noise (S/N) ratio for increasing values of $N$ for the noise data shown in Figure 4.13 . . . . .	43
4.15 A representation of the ideal S/N ratio for increasing distances . . . . .	43
4.16 A representation of the ideal S/N ratio for increasing distances . . . . .	44
4.17 The flux density signal produced after the sensor was subjected to a tilt in the z direction . . . . .	44
4.18 The flux density signal produced after the sensor was subjected to a tilt in the z direction . . . . .	45
4.19 Here we can see that Magnetic Gradient is significantly more stable when the entire system is subjected to the same change in orientation . . . . .	45
4.20 Here that the rabid movement of a single sensor up and down will significantly screw the results produced . . . . .	46
4.21 The stability of the Magnetic Gradient is almost non-existent . . . . .	46
4.22 The magnetic gradient calculated at a sensor distance of 0.3m. Due to the signal monitoring, processing and storage that will be required from any microcontroller that is utilised in this research project, the proposed system is estimated to sample at a lower rate than 2kHz and as a result, aliasing is a concern. This can be addressed however through the use of a gradiometric design which helps negate the effects, and while not entirely successful, is critical prior to digital filter implementation as will be seen below . . . . .	47
4.23 test . . . . .	48
4.24 The result of the magnetic gradient of 4.23, the signal is relatively well defined but the minute measurement of the meteorite of Sensor 2 reduced the effectiveness of the data . . . . .	48
4.25 The effect that an increase in speed has on the compression of the measurement signal. Note that noise is reduced when compared to the similar experiment conductor in Section 4.2. Both experiments were conducted at a height of 6cm at the same location of testing at a sampling rate of 1000Hz . . . . .	49
4.26 Test . . . . .	50
4.27 The Final Sensor Suite CAD Model Before Construction Commenced . . . . .	52
4.28 The Completed Sensor Suite . . . . .	53
4.29 Sensor Suite can also be attached to a pole to ease of carrying, this will enable for the eventual field testing in the event that a drone cannot be sources . . . . .	54
4.30 An example of the data exported by the sensor suite, the layout is identical whether is comes from the myRIO or the Teensy . . . . .	55



# List of Tables

3.1	<i>The Specifications of the FLC-100 [26]</i>	21
3.2	<i>The technical specifications of the FLC-370 [27]</i>	21
3.3	<i>The Varying Characteristics of the Donated Meteorites</i>	23



# Chapter 1

## Introduction

### 1.1 Motivation

verbatim from abstract. ugh.

The detection and identification of Australian meteorites is a task of great scientific interest and due to meteorites being the only significant source of material from other planets and asteroids, are of immense scientific value. New meteorites have the potential to stimulate new research and ideas in cosmo-chemistry, planetary geology, astronomy, and astrobiology. Currently the task of locating meteorites is conducted mostly through visual or hand-held electromagnetic means, meaning that teams of researchers systematically sweep wide areas of potential meteorite landing zones in the hope of finding items of interest.

This research project investigated the deployment of remote sensing technology through magnetic sensors to detect surface or near-surface meteorites in the Australian Desert. Significant cost savings could be achieved if it can be demonstrated that air-born magnetic detection methods can serve as a substitute for some of the ground based techniques or even nominate potential areas for further investigation.

The applicability of this project ultimately goes beyond the autonomous detection of meteorites, rather it establishes a framework for the development of an autonomous science capability which could be implemented across multiple industries. Such functionalities may be applied to Search-And-Rescue (SAR) missions, geological or agricultural inspection, meteorological surveys, and more.

## 1.2 Project Overview

This thesis project looked at comparing various meteorite detection strategies through prior research before focusing on magnetic based detection to consider the development and implementation of an autonomous mobile system for drone assisted meteorite hunting. An investigation was conducted into the feasibility of locating Australian meteorites by magnetic means.

Divided up into three key phases;

- Phase One of the project first looked to establish a feasible framework for the project to justify the initiation of the next two phases. Considerably larger than the other two phases, Phase One ultimately consisted of the design and implementation of various simple sensor test-beds to investigate and determine a viable proof of concept for the project. To estimate the effectiveness of the proposed system and its ability to operate in the field, various environmental factors and constraints were applied to the system. In addition to this, the simulation of the operating conditions also provided valuable knowledge into the effectiveness of the proposed system. Constraints such as various amounts of electromagnetic noise were applied and various algorithms for signal filtering and data acquisition were developed and tested alongside a LabVIEW designed testbed program. Various operating conditions such as drone flight speed, drone height and deployment setup were also established.
- Phase Two saw the development of a complex Sensor Suite test-bed to re-establish and solidify the environmental constraints of the proposed drone deployable system. Various environmental tests were applied to the Sensor Suite to simulate the real-world application of the system. It was in Phase Two that the design of the drone system was considered and the effects of the drone system on the Sensor Suite was simulated in greater depth through the introduction of noise produced by any potential drone system.
- Phase Three saw the construction of the sensor suite, for deployment on a drone chassis, as a completely field deployable, standalone unit and its effectiveness was established through field testing.

## 1.3 Objectives

The following subsections discuss the objectives that were outlined broadly before the start of this research project. A study into the needs of the informal recommendations from the Department of Earth and Planetary Sciences have enabled the construction of clear objectives for the operation and design of the sensor suite. These key objectives have been described in the following sections:

### 1.3.1 Technical Objectives

The overarching technical objective of this research project was the creation of a field deployable sensor suite to detect magnetic anomalies and spatial changes in the magnetic density of a small area to locate ferrous materials near or on the surface of the ground from a low flying aerial vehicle.

In order to achieve this, the following specifications were established;

1. The measurement resolution should be less than 2uT.
2. A data logger should be incorporated into the system with sufficient flash memory capacity.
3. A GPS should be incorporated into the system to provide location points for every cluster of data points. Its resolution should be less than 2m.
4. The mechanical arrangement of the sensor suite should be reconfigurable to change to the number of fluxmeters included in the sensor array
5. The data acquisition rate should be able to reach up to 500 Hz but should provide the ability for the user to change the sampling rate prior to deployment.

To correctly determine the feasibility and operating parameters of this sensor suite, a suitable test bed was required. Various set-ups will need to be constructed to determine the maximum effectiveness for the sensor suite within the parameters defined.

### 1.3.2 Design Objectives

With the primary operational environment being the harsh Australian landscape, the sensor suite will be required to be constructed out of a durable, light weight and robust frame that can travel at some speed at some height.

As such in order to achieve this design goal, the design requirements can be summarised as such;

1. The sensor suite should be portable and lightweight
2. Due to the operational and environmental conditions, it also needs to be robust
3. The materials should allow for the rapid prototyping of the system
4. The sensor suite should feature the ability to be utilised as a standalone unit when not deployed as part of a drone system

### 1.3.3 Research Objectives

The major aim of this research project was to determine the feasibility of using magnetic sensors to locate and detect surface or near-surface meteorites from an aerial vehicle. To meet this critical research objective, an analysis system which can definitively detect potential meteorites within the pre-established limitations will need to be developed.

### **1.3.4 Tasks Outside the Scope of This Project**

This magnetic sensor suite will need to be attached to an unmanned aerial vehicle to retrieve magnetic readings from potential meteorite sites. In addition to this, while the system designed is entirely capable of deployment as a separate system mounted on a drone, its effectiveness will be greatly increased if the sensor suite is deployed as part of a flight control system or configured to allow for the sharing of data. This could potentially lead to a complete system where potential meteorites can be located during deployment not only when the drone has returned and the data processed. Expeditions to appropriate sites will also need to be organised. These expeditions will need to be undertaken with collaboration with a third party and, along with the complete design and construction of a suitable drone chassis, are not included in the scope of these research project. Suitable drone bodies and their respective attributes have been considered however throughout the completion of this research project.

# Chapter 2

## Literature Review

### 2.1 Meteorites

#### 2.1.1 Justification

The third time? That's looking lazy

The detection and identification of Australian meteorites is a task of great scientific interest and due to meteorites being the only significant source of material from other planets and asteroids, are of immense scientific value. New meteorites have the potential to stimulate new research and ideas in cosmo-chemistry, planetary geology, astronomy, and astrobiology.

#### 2.1.2 Current Methods of Meteorite Detection

As it currently stands, the most common method for the location of meteorites is through visual or hand-held electromagnetic means, meaning that teams of researchers systematically sweep wide areas of potential meteorite landing zones in the hope of finding items of interest. This is both labour and resource intensive with a limited potential for a return of investment. However, these methods are incredibly limiting in regards to the environments that they can be deployed as they become exponentially less effective as the amount of surrounding terrestrial rock increases, [2] And it is due to environments such as these that we can see the implementation of more sophisticated instruments for meteorite detection.

Magnetic sensors are routinely used to locate iron, stony iron and ordinary chondrite meteorites around the world [1] [2]. However, while these methods are considered effective when used to locate iron, stony iron and ordinary chondrite meteorites, there are many scientifically valuable meteorites that contain few ferromagnetic minerals. Martian and lunar specimens usually fall under this category and are ultimately indistinguishable from terrestrial rocks using sensors. As such, methods such as multi-spectral imaging and ground penetrating radar have also been used to aid in the search for meteorites in Antarctica [3] [4] [5]

One of the primary goals of this project will be the successful identification of me-

eteorites when terrestrial rocks are present. As mentioned previously, the presence of iron-nickel is an important characteristic of most meteorites, not only does their composition ensure that they are relatively magnetised, these meteorites are also considerably denser than the surrounding environment [1].

### 2.1.3 Attempts at the Autonomous Detection of Meteorites

When one attempts to collate information regarding the detection of meteorites by autonomous means, the Carnegie Mellon University's Robotic Antarctic Meteorite Search (RAMS) is always referenced as a primary source material. Through their development and implementation of a mobile robotic system (Nomad) deployed with a meteorite detection sensor suite, they provided an ideal demonstration of autonomous robotic based meteorite detection. This culminated in the events of January 2000 when Nomad made the first autonomous classification of a meteorite by robotic means [3]. While considered a success [6], it was noted that due to operational and mechanical limitations, the expedition ultimately showcased the difficulty of effectively deploying complex sensors in such a hostile environment, as well as highlighting the limited performance in the speed and coverage of autonomous search [6].

Airborne and/or satellite hyper-spectral imaging has also been routinely employed to aid in the detection of surface meteorites [7]. Routinely implemented as a detection method for various materials and the mapping of their distributions across the landscape, airborne hyper-spectral imaging has been used in a variety of applications and industries. However, this method of detection has however been almost entirely limited to locating geography that is better suited to the manual search for meteorites [8] rather than direct meteorite detection.

In 2014 an undergraduate research project was conducted and funded by the University of Southern Queensland [4] where the use of hyper-spectral imaging from an unmanned aerial vehicle (UAV) to search for meteorites was investigated. This research thesis has been the only case of autonomous aerial meteorite detection that was found to have occurred. In addition, while this project required the development of an image and position logging system for determining potential meteorite locations, the development and implementation of the Unmanned Aerial Vehicle was outside the scope of the research project [4].

Its a good review, not great, but you found all sources for yourself.

## 2.2 The Viability of the Australian Landscape

I can answer that. The  
australian landscape is  
highly viable.

Australia is one of the most viable locations on Earth to launch expeditions to discover new meteorites outside of Antarctica [9]. (Antarctica accounts for almost 50% of all recovered meteorite locations worldwide [1]). It is important to note that meteorites are just as likely to fall anywhere else in the world as they are in both these locations, it is just that using current methods, deserts offer unique conditions that promote the identification of potential meteorites. This is ultimately because currently, the most effective method of

detecting meteorites is by eye, teams of human researchers form a line with tens of meters between each person. The team then moves in unison to visually detect meteorites on the ground, and it is through this method that a potentially viable area can be systematically searched.

$3.8 \times 10^6$  km<sup>2</sup> of the Australian continent comprises of deserts or semi-arid land (50% of the landmass) [10], most of which provide suitable conditions for the detection and the prolonged preservation of meteorites. Two particularly critical areas containing concentrations of meteorites have been recognised as the Nullarbor Region of Western Australia and Menindee Lakes in western New South Wales [9]. And of these regions, more than 50% of the total number of documented Australian meteorites had been recovered from Nullarbor Basin [9]. The sedimentary basin that makes up the Nullarbor comprises essentially of limestone, which, due to its light appearance provides a high visual contrast between the black or dark coloured meteorites [11], this is further compounded by the lack of vegetation and large terrestrial rocks. More so, due to the lack of moisture and a temperate climate, [9] specimens are much better preserved as iron meteorites do not rust and stony meteorites weather much slower.

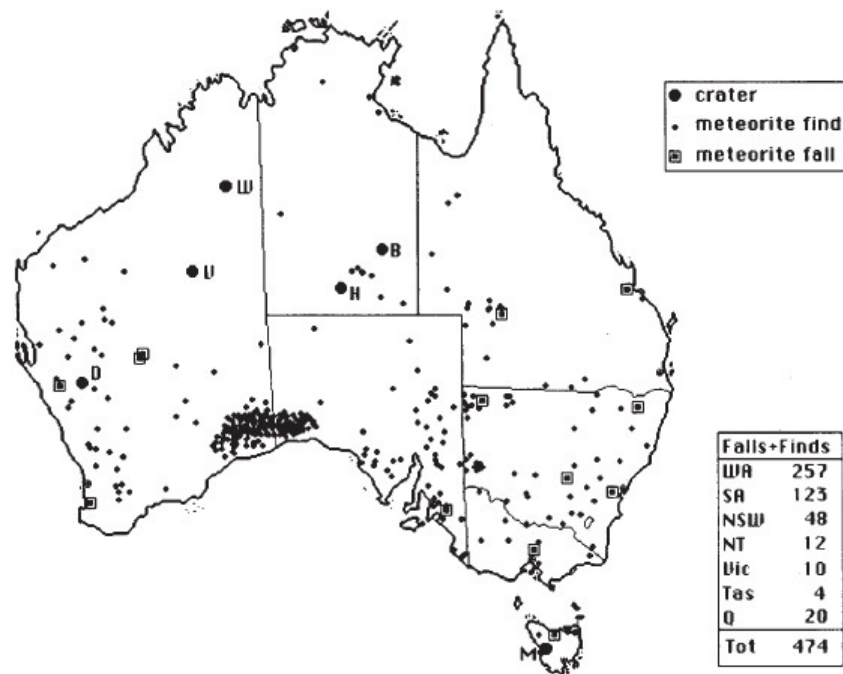


**Figure 2.1:** Geographical distribution of meteorite finds and observed falls in Australia. While accurate at depicting the prevalence and locations of meteorite finds across Australia, due to the publish date of the data, (1996) there has been a considerable increase in the amount of finds across these regions.

In addition to this, there is significant evidence to suggest that meteorites are still lying on the surfaces on which they fell and that geologically, the region has remained undisturbed for close to 30,000 years [11]. It is for these same reasons that Antarctica

so where in australia would you go looking if you had an awesome mag sensor suite?

is the ideal location for meteorite hunting [12], more isolated and desolate than even the Australian desert, it provides the perfect conditions for the prolonged preservation of meteorites. It is due to this that more meteorites have been found in Antarctica than the rest of the world, and why a significant proportion of the literature available focuses on the Antarctic Search for Meteorites (ANSMET) and on Antarctic meteorites in general.

## 2.3 Magnetic Materials

### 2.3.1 Understanding Magnetic Fields

A basic understanding of magnetic fields and their nature is fundamental to understanding the decisions, techniques and methods utilised in this research project.

A magnetic field  $\vec{H}$  is measured as a vector quantity, consisting of both a magnitude and direction. The magnetic field can be visualized as magnetic field lines with one of the most familiar sources for this visual representation being the bar magnet, as shown below:

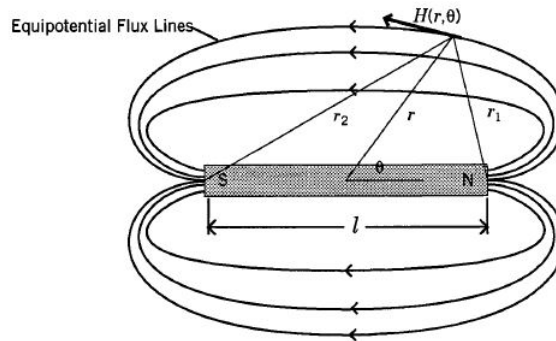


**Figure 2.2:** A magnetic field is a vector quantity with both magnitude and direction properties [13]

what's a measurement source?

The relationship between magnetic field  $\vec{H}$  and the distance from the measurement source can be related through the following equation:

$$H = \frac{3(\vec{m} \times a_r)a_r - \vec{m}}{r^3}$$

is this equation valid for all space? Where is your origin? Perhaps it is only valid if  $r$  is much larger than the magnet?

Where  $a_r$  is the unit vector along  $r$ ,  $r$  is the distance between the magnetic source and the measurement point, and  $m$  is the magnetic dipole moment.

The strength and intensity of this magnetic field is known as magnetization  $\vec{M}$ , which is also quantified as a vector and defined as the moments per unit volume. The third magnetic vector  $\vec{B}$ , is referred to as flux density or magnetic induction. [13] Flux refers to the flow of energy through a surface, with the term applying to any a magnetic field in the field of electronics. While magnetic flux density  $\vec{B}$  is simply the measurement of the strength of a magnetic field in terms of the density of magnetic flux per unit area,

magnetic field  $\vec{H}$  represents the magnetic field strength which is a measure of the force without any material medium. [14] It is the complete force due to the magnetic field that is being generated.

In free space, magnetic flux and magnetic field strength are proportionally related to each other through  $\mu_0$ , with that being the magnetic permeability of space.

$$B = \mu_0 \text{ missing H} \quad (2.2)$$

When discussing a material's magnetic response however, the relationship can be described as:

$$B = \mu_0(H + M) \quad (2.3)$$

Magnetic materials can also be loosely classified as either magnetically hard or soft, with the former being used to describe objects permanently magnetised, and the latter for any object that can have a magnetic field induced. [13] All ferrous objects will have some sort of magnetic field; however, most are so minute that they are categorised as a magnetically soft material.

### 2.3.2 Magnetic Gradient

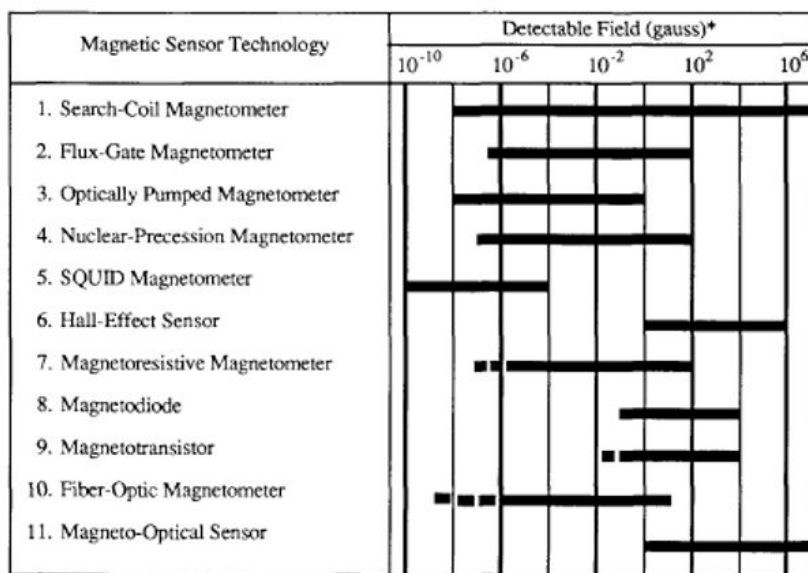
The measured difference in magnitude or direction of a magnetic field  $H$  or magnetic flux density  $B$  between two or more points in space can be described as the magnetic gradient. This Gradient  $G$  can be defined as the change in magnetic flux  $\Delta B$  divided by the change in distance between the points  $\Delta d$ .

OK, that is an find summary of magnetic fields. You started with a bar magnet, maybe you could describe how it is alike or different to a meteorite?

### 2.3.3 Magnetic Sensors

The application of the magnetic sensors discussed for this project are to measure spatial changes in the magnetic field of a small area to locate ferrous materials near or on the surface of the ground from a low flying aerial vehicle.

There are two types of Magnetic field sensors and these are categorised by their field strengths and measurement range. The first being Magnetometers which measure low electric fields ( $< 1mT$ ) and Gaussmeters which are used to measure high fields ( $> 1mT$ ) [13]. Magnetometers can be further divided by their magnitude types, these being vector and scalar (**Figure 2.4**). Due to the low strength of the electronic field produced by any potential meteorite samples, Fluxgate magnetometers are proposed as a most effective detection method and as such were chosen for this research project.



\*Note: 1 Gauss =  $10^{-4}$  Tesla

**Figure 2.3:** An assortment of magnetic sensor technology and their respective sensing ranges [16]

#### Magnetometers

When considering the available magnetometers, there are two different types; these being scalar and vector. The former which are also known as total field sensors, measure the magnitude, but not direction, of an electric field and the latter, which measures a single component of the magnetic field vector. [13] Total field magnetometers have an advantage as the measured output is not dependent on the sensor orientation, however they must be aligned with the ambient field in order to operate effectively, and this severely reduces their practicality for a drone deployable system.

Induction coil and fluxgate magnetometers are considered the most common vector magnetometers. Widely used for compass navigational systems since 1928, [16] they have

a high resolution for the measurement of weak magnetic fields and are widely used for the measurement of the Earth's Magnetic Field. [17] As such, when considering potential magnetometers for use in this project, they presented a highly desirable choice.

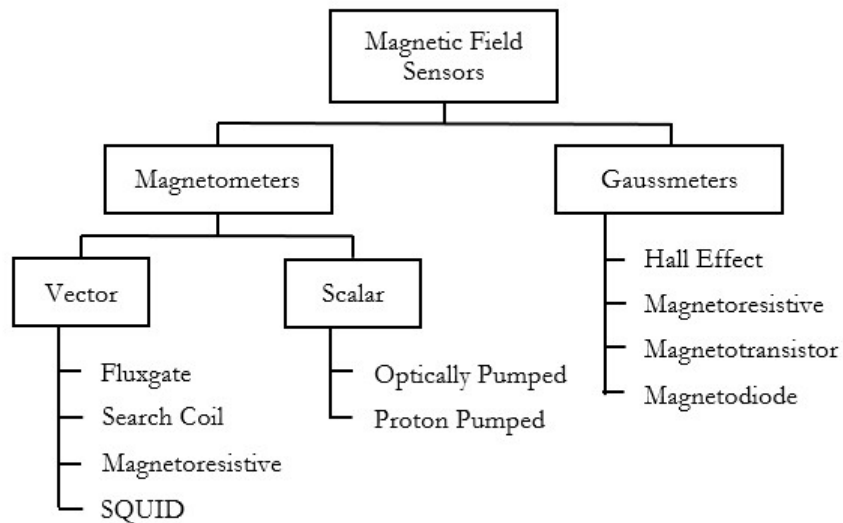


**Figure 2.4:** Magnetic Field Sensors are categorised into two distinct types based on their magnetic field strengths and their measurement ranges. With magnetometers measuring low fields and gaussmeters measuring high magnetic fields, magnetometers were the obvious choice for this research project.

it is not an electronic field!

Due to the low strength of the **electronic** field produced by any potential meteorite samples, and the assumption that magnetic susceptibility being the primary method of meteorite detection, Magnetometers are proposed as the most effective detection method for this research project. In addition, there is a considerable amount of information available [18] [6] [3] [2] and magnetometers are already considered a viable tool in meteorite identification and geospatial surveillance. Furthermore, the measurement of the metal content will not only help identify a potential meteorite, but should it be successful, may allow for the classification of meteorite without destroying the integrity of the sample.

### Fluxgate Sensors

Considered to be one of the most widely used types of magnetometers [17], fluxgate magnetometers measure the intensity and orientation of magnetic lines of flux. Fluxgate magnetometers have numerous desirable advantages over other magnetometers with the most common outlined below:

- They are physical small and light
- Robust and reliable
- Require very little power to operate with a low current consumption

- Traditionally have low noise and high stability of output signal
- High Frequency

The operation of a fluxgate magnetometer is dependent on a transducer that converts a magnetic field into an electric voltage. Based on Faradays laws, with this law stipulating that if any loop of wire is subjecting to a change in magnetic flux  $\phi$ , then some voltage will be induced in the loop that is proportional to the rate of change of the flux [13].

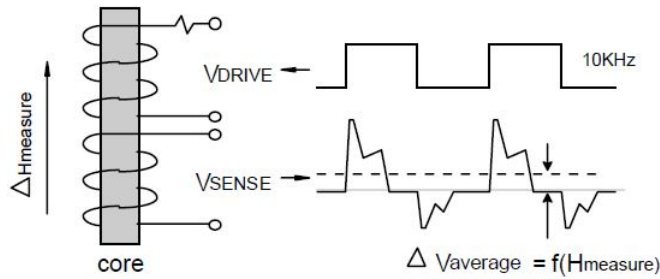


**Figure 2.5:** Operation of a Fluxgate Magnetometer Coil

This change in flux can be represented as such;

$$e(t) = -\frac{d\phi}{dt} \quad (2.4)$$

Hence, as the loop has some surface area  $A$ , this change in magnetic flux  $\phi$  can be directly tied to the  $B$ , the magnetic flux density to measure the terminal voltage of a magnetically induced field.

$$e(t) = -\frac{d(B \times A)}{dt} \quad (2.5)$$

This can then be further expanded upon to incorporate the component of the magnetic field  $H$  being measured, thus, the voltage at the terminals of the signal winding can be represented as such:

$$e(t) = nA \frac{d(\mu_e \mu_0 H)}{dt} \quad (2.6)$$

Where  $H$  is the magnetic field,  $n$  the number of turns on the signal winding,  $A$  the cross-sectional area and  $u(t)$  the permeability of the winding core [13].

All of this comes as a complete package in a fluxgate magnetometer and once provided the necessary voltage required, it will traditionally output a voltage proportional to magnetic field being measured.

good section that is

### 2.3.4 Magnetic Gradiometers

While the output of vector magnetometers is dependent on their orientation, their sensitivity can be greatly improved by two (or more) precisely aligned vector sensors at some distance apart. Known as a differential or gradiometer configuration [19], this is a standard practice in the deployment of vector magnetometers and the best considered method for robotic deployment. This is because gradiometers measure the magnetic field gradient as opposed to the total field strength, which allows for the removal of background noise.

Consisting of pairs of fluxgate magnetometers that are at some distance apart, the readings are subtracted to measure the difference between the magnetic field measurements which provides the field gradients caused by magnetic anomalies [18]. Not only does this allow for the compensation of the noise through electromagnetic interference, but will also allow for the compensation of the variability in earth's magnetic field. [19] The premise being that this configuration should dramatically increase the sensitivity of detection methods.

As was outlined in *Subsection 2.3.2*, the difference in the magnetic field measured at the two points is divided by the distance between the detectors to determine the electromagnetic field gradient between them. Due to the use of fluxgate sensors, such a gradiometer throughout this research project will comprise of two coils, which are arranged at an horizontal distance from one another and which are electrically connected in series. The coils are thus arranged so that their respective coil planes lie parallel to one another.

According to this system, magnetometers are brought close together and the difference in the measurements at each instrument is obtained. If the distance between the two magnetometers is kept constant, this difference provides a magnetic gradient which indicates the presence of magnetic anomalies and is unaffected by environmental variations.

### 2.3.5 Applications of Gradiometers

In addition, it has been shown that there are numerous benefits that magnetic gradient measurements bring to geophysical surveys [20] [21] [22], both airborne and surface [23].

These benefits can be outlined as such:

- Higher Resolution
- Minimising of Aliasing
- Ease of Interpretation
- Insensitivity to Magnetic Variations
- Insensitivity to Rotational Errors

These benefits are further outlined in *Subsection 3.5.3* where a dual fluxgate gradiometer is compared to a single fluxgate sensor and a total field sensor.

## 2.4 Digital Signal Processing

### 2.4.1 Digital and Analogue Filters

When it comes to Digital Signal Processing, one of the most powerful and commonly applied tools is the use of digital filtering [24]. Digital filtering allows not only for the elimination of errors in the signal associated with passive component fluctuations or noise, but they also allow for the application of various performance specifications that would be otherwise impossible with to achieve with the implementation of analogue filters. However, the most important and fundamentally defining feature of a digital filter when compared to an analogue filter is simply the ease of which their characteristics can be changed or adapted to certain situations via software control. Hence they are widely used in any application that requires the manipulation of a signal, most commonly, for noise cancelation. Digital filters share the same fundamental characteristics of analogue filters, this being the characterisation of the desired filter response followed by the calculation of the filters parameters [24]. Their key difference are the values that are provided by the filter for processing, for analogue filters, these values are calculated in terms of resistance, capacitance and inductions while digital filters produce coefficient values that reside in memory to be utilised by the digital signal processor [25]. To apply a digital filter to any analogue value sent from the sensor, an Analogue-to-Digital Convertor (ADC) needs to be utilised, this was of no issue however as any microcontroller that offers analogue I/O capabilities has an ADC inbuilt.

# **Chapter 3**

# **Project Methodology**

## **3.1 Methodology Introduction**

This chapter of this report will outline the methodology adopted to achieve the timely completion of this research project.

## **3.2 Project Considerations**

The following subsections will attempt to illuminate the various solutions, materials and equipment that were considered before the initiation of this research project. Various design ideas were considered before a broad solution was selected and implemented. As will be seen throughout this document, these initial considerations will evolve into a more flexible and robust solution.

### **3.2.1 Sensor Suite**

The various sensors will need to be validated and tested in combined laboratory and field tests on a variety of stony and iron meteorites. Experiments will need to be conducted to show if one or both sensing modes will achieve comprehensive readings from meteorites. Data will be collected using real meteorites ranging in size and of various iron content. These meteorites will also need to be tested at various heights and speeds above a standard medium.

### **3.2.2 Data**

The data collected will need to be stored and processed into a format that will allow for the best possible study both during this project and into the future. The data will need to be collected in such a way that modelling tools, data processing software and techniques will be improved with the ultimate purpose of better design of the testing equipment and interpretation of experimental results. Requirements and standards for data generated from physical tests will be identified, for calibration and development of different numerical models.

### **3.2.3 Noise**

The sensor suite will need to be configured to allow in-situ autonomous calibration and to ensure that noise is mitigated from the electrical components of any potential robotic body. Noise and calibration will be significant issues in the robotic deployment of magnetic and eddy current sensors. Electric motors in the propellers will contribute significantly to the ambient magnetic field. Microprocessors, radio communications and power supplies have the potential to generate substantial RF interference should they not be insulated correctly.

### **3.2.4 Preparation for UAV Deployment**

A particularly challenging and complex subset of autonomous mobile systems is an autonomous Unmanned Aerial Vehicles (UAVs). These systems can be affected by external disturbances, require high bandwidth control and available sensing is limited by the payload capacity of the vehicle. At the same time the missions envisioned for the deployment

of these sensors are very challenging, involving low-altitude flight over potentially obstacle strewn terrain.

### 3.2.5 Materials

In order to construct a sensor suite that can be deployed underneath a drone chassis it was immediately determined that light and robust materials would need to be used in order to keep weight at a minimum. Any sensor suite would also need to be field deployable by hand held means in order to test its effectiveness.

### 3.2.6 Project Scope

From the research conducted, it was determined that the use of a magnetic gradiometer array was the ideal solution for the requirements of this research project. This can be further seen through the testing conducted in **Subsection 3.5.3**. It was also decided that the gradiometer array would be spread out horizontally and not vertically, the benefits of this would be twofold; the first being that the advantages of a Gradiometric configuration greatly improve a traditional magnetometer configuration, and two, that the total surface area that would be surveyed would be increased.

It was also determined that electrical noise and interference would be a considered hindrance on the project, and the closer it was located to an interference source the worse it would be, as such it was determined that the sensor suite would need to be designed such that it was located on a boom with sufficient distance from the drone unit.

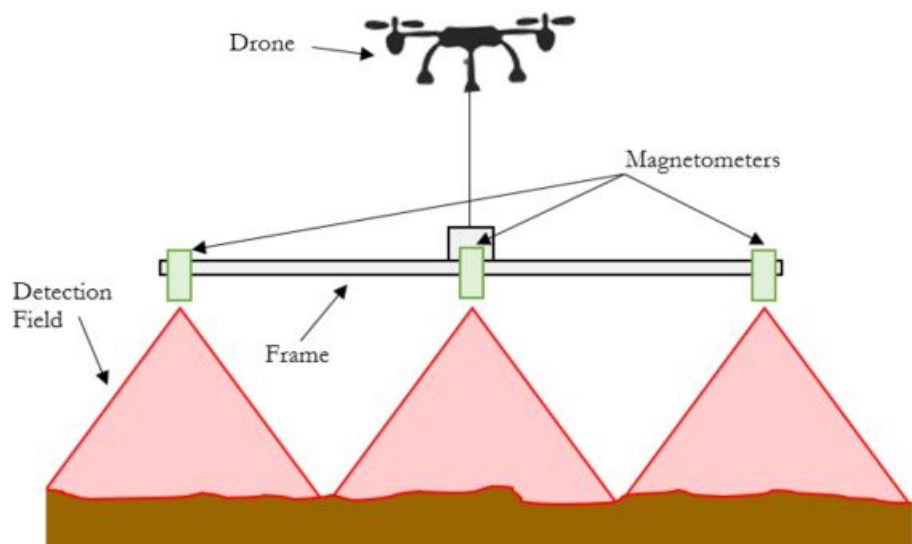


**Figure 3.1:** The Intended Design of the Sensor Suite from Research Conducted

## 3.3 Resource Requirements

It was established from early on that there would be a significant amount of material required for this project to be successful. As the budget of the project was limited, it was decided that donations or loans would be the primary source of hardware and any additional materials could be purchased at a later date.

### 3.3.1 Hardware

#### Microcontroller: Teensy 3.2

The Teensy 3.2 from PRJC is a complete USB-based microcontroller compatible with the Arduino IDE. Designed with a small footprint when compared to other microcontrollers of the same calibre, it also can be programmed in C or with Arduino IDE, which runs on Windows, Macintosh OSX, and Linux operating systems [26].

A summary of the highlights of the Teensy 3.2:

- All programming is done via the USB port.
- The Teensy can emulate multiple devices without the need of expensive additional integrated circuitry.
- Extensive code examples and classes available.
- The board is very affordable (\$17 USD).
- Comes with analogue, digital, audio and power I/O of which there are a significant number of analogue input pins (21).

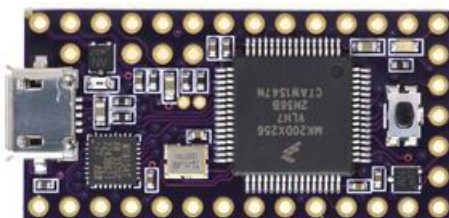


**Figure 3.2:** While the Teensy 3.2 still used the standard 0.1inch pin spacing for breadboarding, it also features SMD headers on the underside allowing for over 34 I/O Pins

Ultimately however, there were three main reasons for the use of the Teensy 3.2 for the initial prototyping of the sensor suite. The first being the significant number of analogue inputs required by the various magnetometers and the later two being the miniature footprint and lack of additional hardware required for operation. While the Teensy 3.2 wasn't the primary microcontroller used throughout this research project, as the functionality of the myRIO was unmatched (see 3.3.1), should this project eventually be implemented

on a drone platform the teensy will be the obvious choice of microcontroller due to the extensive cost, size and weight of the myRIO. It is for this reason that the functionality of the sensor suite was also programmed and implemented in the Arduino IDE and can be found in *Appendix A.1*.

The Teensy 3.2, when compared to other similar microcontrollers such as the Arduino UNO, presents itself as a clear choice for any moderately experienced programmer operating in a rapid prototyping environment.

### Microcontroller: myRIO

The myRIO from National Instruments (NI) is a portable reconfigurable microcontroller that allows for the design and control of various robotics and mechatronics systems. Designed for use with the LabVIEW system design software, it unfortunately provides an incredibly expensive solution when compared to the Teensy 3.2. However the benefits of both the myRIO and the LabVIEW Software (*see section ??*) cannot be understated.

Consisting of a ARM Cortex-A9 duel core processor, a reconfigurable Xilinx FPGA, various analogue and digital inputs and outputs, and the graphical 'function-block' style LabVIEW software, the NI myRIO provided the ability to rapidly create custom circuitry with high-performance I/O and flexibility [27].



**Figure 3.3:** Consisting of 10 analogue inputs, 6 analogue outputs, audio channels, and 40 digital input/output (DIO) pins. The NI myRIO also includes an on-board WiFi module, a three-axis accelerometer, and several LEDs.

nice summaries of the two controllers

DIO15 / I2C.SDA	34	33	+3.3 V
DIO14 / I2C.SCL	32	31	DIO10 / PWM2
DGND	30	29	DIO9 / PWM1
DGND	28	27	DIO8 / PWM0
DIO13	26	25	DIO7 / SPI.MOSI
DGND	24	23	DIO6 / SPI.MISO
DIO12 / ENC.B	22	21	DIO5 / SPI.CLK
DGND	20	19	DIO4
DIO11 / ENC.A	18	17	DIO3
DGND	16	15	DIO2
UART.TX	14	13	DIO1
DGND	12	11	DIO0
UART.RX	10	9	AI3
DGND	8	7	AI2
AGND	6	5	AI1
AO1	4	3	AI0
AO0	2	-	+5V

**Figure 3.4:** The pin layout of the myRIO's MXP identical connectors A and B

### Magnetometer: FLC-100

The FLC-100 Single-Axis Field Sensor from Stefan Mayer Instruments, is a miniature fluxgate magnetometer with a high sensitivity [28]. Designed to measure weak magnetic fields of up to 100 uT, it provided the perfect sensor for the applications required for this research project. Designed as a complete system that works without any external circuitry, once provided the required voltage the analogue voltage outputted is proportional to the magnetic field parallel to the detection coil.

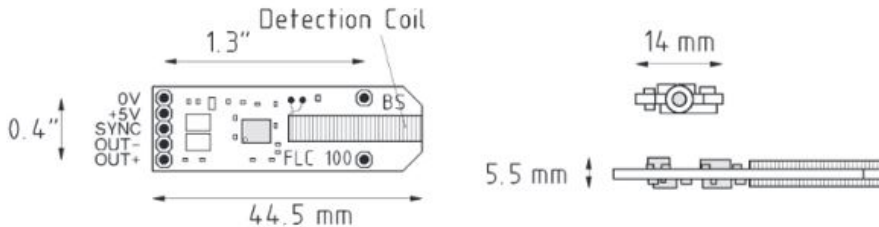


**Figure 3.5:** The design specifications of the FLC-100

Due to the low current consumption and voltage, the FLC-100 was ideally suited for the battery powered sensor suite. In addition, the sensor also featured the ability to synchronise its excitation frequency with any other FLC-100 connected in series to its SYNC pin. A total of five units were donated by the Department of Earth and Planetary Sciences.

<b><i>FLC-100 Specifications</i></b>	
Measurement Range	$\pm 100 \mu T$
Accuracy at 20°C	$\pm 2\% \pm 0.3 \mu T$
Operating Temperature	-40°C to 85°C
Supply Voltage	5V $\pm 5\%$
Output Voltage	$\pm 1V/50 \mu T$ , max $\pm 2.5V$
Supply Current	$\approx 2mA$
Bandwidth	0 to 1kHz

**Table 3.1:** *The Specifications of the FLC-100 [26]*

### Magnetometer: FLC-370

The magnetic field sensor FLC-370 is a triaxial miniature fluxgate magnetometer designed for the measurement of weak magnetic fields up to 200 $\mu T$  produced by Stefan Mayer Instruments [29]. As with the FLC-100, it was donated by the Department of Earth and Planetary Sciences.

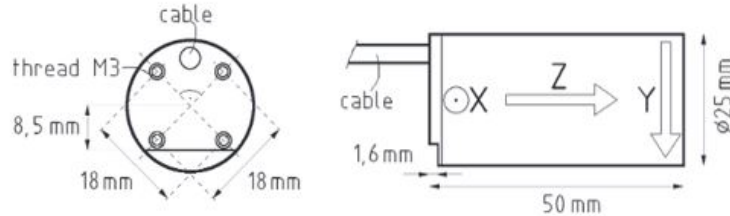


**Figure 3.6:** *The design specifications of the FLC-370*

Unlike the FLC-100 however, the FLC-370 was a complete triaxial fluxgate magnetometer with three analogue output voltages proportional to the X, Y and Z components of any measured magnetic field.

<b><i>FLC-370 Specifications</i></b>	
Measurement Range	$\pm 200 \mu T$ at 12V
Accuracy at 20°C	$\pm 1\% \pm 0.5 \mu T$
Accuracy of Measurement Angle	$\pm 1\%$
Operating Temperature	5°C to 125°C
Supply Voltage	4.8V to 12V DC
Output Voltage	$\pm 1V/35 \mu T$ , max $V_+/2$
Supply Current	$\approx 6mA$
Bandwidth	0 to 1kHz

**Table 3.2:** *The technical specifications of the FLC-370 [27]*

### GPS Receiver: LS20031

The LS20031 GPS receiver from LOCOSYS Technology Inc. is a complete GPS package that includes both an embedded antenna and the required GPS receiver circuits [30]. A low-cost and low-weight module, the LS20031 operates at 5hz but can be increased to 10z. The LS20031 can track up to 66 satellites and due to its low power consumption and sufficient sensitivity and performance, it provided an ideal choice when selecting a GPS unit within modest budget constraints



**Figure 3.7:** The design of the GPS smart antenna module, LS20031 [28]

Features Include [28]:

- 5Hz – 10hz output
- 57600bps TTL serial interface
- 3.3V @ 41mA
- 66 Channel
- Built-in micro battery to preserve system data for rapid satellite acquisition
- LED indicator for fix or no fix

The LS20031 supports the NMEA 0183 protocol and as such did not require too much effort to integrate into the LabVIEW software environment. **ThIn** summary of this section, it was found that the while update rate is configurable up to 10Hz, the LS20031 is most reliable at the default rate of 5Hz and any increase in the output frequency can have severe effects on sensitivity.  $\approx < 2m$  variance @5hz while  $> 3m$  variance @10hz

OK, good you figured that out and reported it here.

## 3.4 Meteorite Testing Samples

In order to develop a system that could differentiate between meteorites and the surrounding terrestrial environment, several meteorite samples were donated. These samples are pictured in *Figure 3.8*.



**Figure 3.8:** The Five Meteorites Donated by Craig O'Neill of the Department of Earth and Planetary Sciences

The meteorite samples were comprising of different sizes and weight with various weathering grades, in addition, two had cleanly cut and polished faces and crusts and only one (M2) was a complete specimen, there were all however part of the iron category of meteorites. M2 would end up being the baseline meteorite for the remainder of this research project due to the quality of the specimen and because it was a prime example of the types of meteorite this project was attempting to locate.

<b>Meteorite Characteristics</b>	
M1	Offcut
M2	Complete
M3	Offcut
M4	Fragment
M5	Fragment

**Table 3.3:** The Varying Characteristics of the Donated Meteorites

## 3.5 Sensor Test-Bed Development

### 3.5.1 Simulation of Operating Conditions

The test beds and prototyping structures outlined in this section were designed to simulate the passing of magnetic objects beneath the sensor suite in order to assess its performance for eventual implementation on a low altitude drone. It was decided that the most efficient low-cost method to represent this in a controlled environment was through the use of a conveyor system that would travel at certain speed underneath a stationary mounted sensor. Meteorites and other ferrous object could be placed or mounted on this belt to travel past the sensor at some speed in order to ascertain the effectiveness of measuring the magnetic field of the object and later, the magnetic gradient.

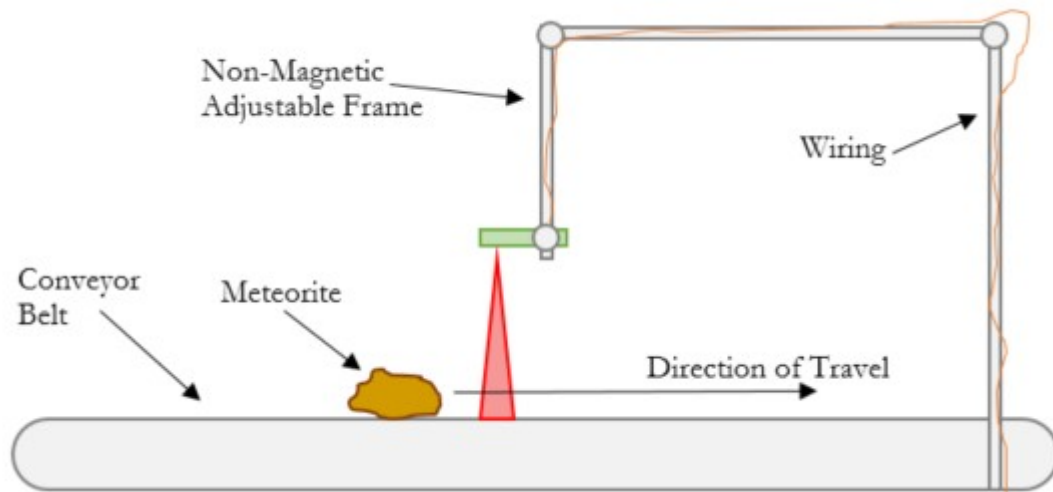


**Figure 3.9:** The Initial Design Prototype of the Sensor Test-Bed

In order to establish the initial goal of simply assessing the feasibility of this research project, the design and construction of the first prototype also aimed to provide the following functionalities:

- Ensure that the sensor was kept level during testing
- Provide a stable and robust non-metallic structure
- Allow for the raising and lowering of the sensor quickly and efficiently
- Allow for the rotation of the sensor
- Ensure that sensors could be removed and replaced without any deconstruction of the scaffold

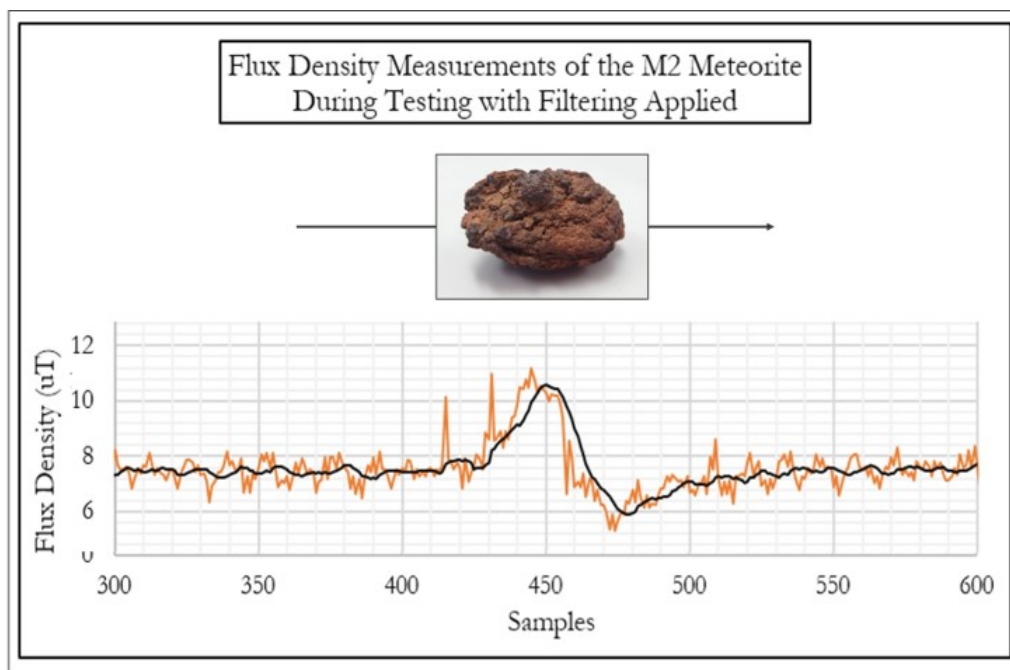


**Figure 3.10:** *The basic premise for establishing the feasibility of this research project*

- Should the deconstruction of the test-bed be required, it could be done easily and with minimal effort while maintaining the basic structure so it could be put together with ease at a later stage.

A simple treadmill was generously donated by the Macquarie University Speed Team and was used extensively until the construction of the initial sensor suite prototype much later in the project.

### 3.5.2 Mechanical Design

The first prototype of the sensor suite was constructed out of PVC pipe and mounted on a camera tripod. This simple system could be easily rotated, raised, lowered and inclined at will with a turn of one of the wheels located on the tripod. The levelling bubbles on every axis also ensured that the pipe holding the sensor was kept straight and level.

These materials also ensured that there was no ferrous object close enough to the sensor suite to induce any noise or a bias signal during the subsequent testing. The simple effectiveness of the test-bed ensured that it was liberally used throughout the research project.

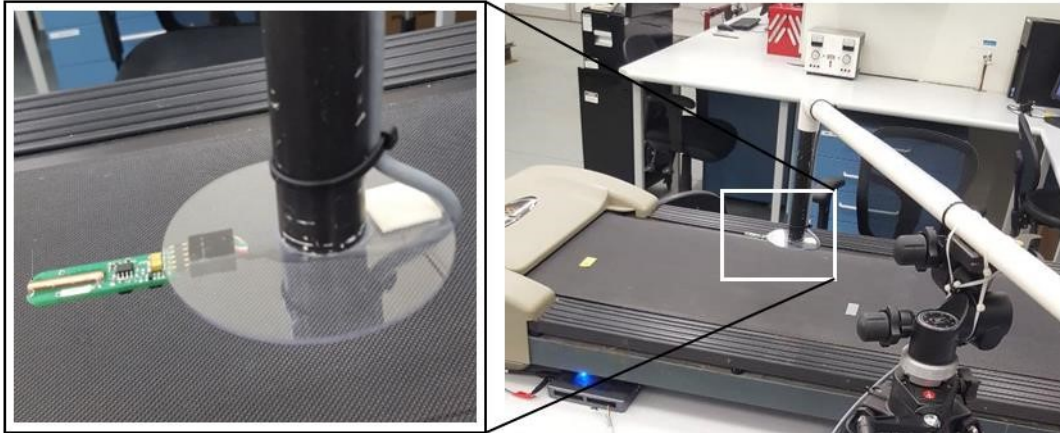


**Figure 3.11:** The initial test bed for a single FLC-100 sensor

### 3.5.3 Gradiometer Implementation

Below is an illustration of the gradiometric or differential set-up of the sensor test-bed, it is important to note that great care must be taken to ensure that the sensor coils are kept parallel to reduce the variation between measurements. This highlighted in further sections where the effects of sensor pitch and yaw are quantified and discussed.

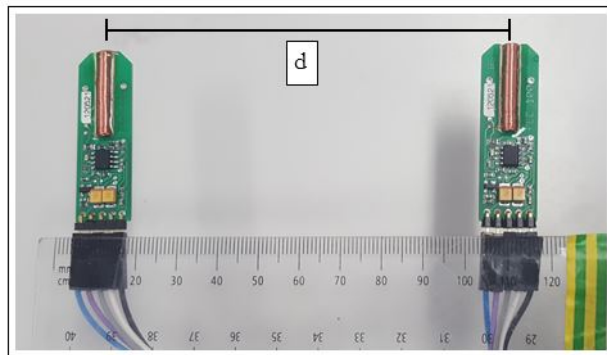
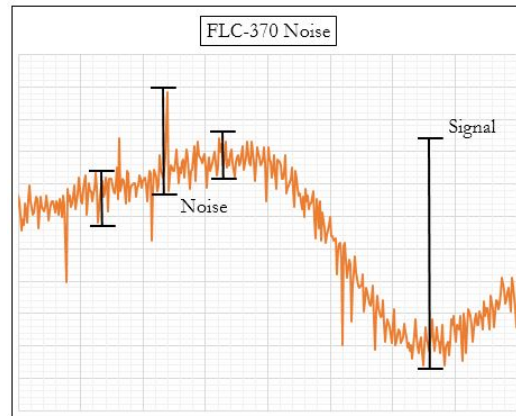


**Figure 3.12:** The standard implementation of a gradiometric setup for testing, this was fixed to the sensor mount seen in Figure 3.11 and was the method used for all gradiometric calculations

## 3.6 Signal to Noise

All instrumental methods are limited by both accuracy and precision, this is ultimately due to all techniques being physical measurements. This accuracy and precision are limited by the size of the transducer which will be limited by the parameters that it is intending to measure.

The figure below illustrates the noise that is imposed on a signal taken from the FLC370. The noise is a measure of precision and thus the reduction of its influence on the signal is highly desirable. There are a number of methods that can be used to influence the Signal to Noise (S/N) ratio.



This does not define how you calculate the SNR for your signals.

**Figure 3.13:** Example of a FLC-370 signal containing noise

As was outlined above, signal processing involves the physical or digital methods for the manipulation of data to enhance the S/N ratio. Physical methods relate to the analogue manipulation of the data, physical methods implemented throughout this research project involved:

- Analogue Filtering (through the syncing of analogue excitation frequencies)
- Grounding
- Bandwidth Modulation

There are numerous digital methods that are available, but the digital filters implemented included:

- Moving Average Filters
  - Unweighed Moving Average Filter
  - Multiple Pass Moving Average Filter
  - Boxcar Filter
  - Kernel Filter
  - Savitzky-Golay Filter
- Fourier Transforms

### 3.6.1 Digital Signal Processing

#### The Moving Average Filter

A moving average filter is one of the simplest FIR filters that can be applied to a signal and it is an incredibly popular method for smoothing data [33]. As the name suggests, this filter works by averaging a number of sampled points from the input signal in order to produce a new filtered point. Mathematically, it is represented as follows;

$$y[i] = \frac{1}{N} \sum_{j=0}^{N-1} x[i-j] \quad (3.1)$$

Where  $x[ ]$  is the input signal,  $y[ ]$  is the output signal and  $N$  is the filter length or number of points averaged over one side of the output sample. For example, a moving average filter of filter length  $N$  is given by:

$$y[5] = \frac{x[5] + x[4] + x[3] + x[2] + x[1]}{5} \quad (3.2)$$

It is important to note however the first values of data cannot be utilised by this method and are dumped post processing as they are still raw data elements. Alternatively, a filtered data point can be chosen by implementing this method symmetrically, i.e. choosing a group of points which surround the value. Mathematically this is represented by;

$$y[i] = \frac{1}{N} \sum_{j=-\frac{N-1}{2}}^{\frac{N-1}{2}} x[i+j] \quad (3.3)$$

If we implemented the same data as above using the symmetrical method, we would see;

$$y[5] = \frac{x[3] + x[4] + x[5] + x[6] + x[7]}{5} \quad (3.4)$$

#### Implementation of the Moving Average Filter in Code

One of the greatest advantages of the moving average filter is that it can be implemented in code incredibly fast due to its recursive nature[34]. The indexing scheme utilised is also incredibly simple and allowed for the maximum use of recursion as the sum of the values in the array had already been calculated and so it was a simple process of subtracting the previous value and adding the new value to this sum.

However since a sampling rate of 1kHz was desired, the decision was made to not include a visual UI where the plotting of the data could be seen. While this would have been a nice feature, there was no need for it to be implemented as the filtered data could be outputted post processing into excel where it could be graphically represented.

### Savitzky-Golay Filter

The Savitzky-Golay is an digital filter where the basic premise is to convolute the digital signal by fitting successive sub-sets of adjacent data points with a 2nd degree polynomial [37]. In essence, when the data points are sampled at equal spacings, a single set of convolution coefficients can be determined through an analysis using the least-squares equations.

One of the more popular methods for the processing of the signal is to replace each value of the series with a new value that is determined from a polynomial fit of  $2n+1$  to their neighbouring points (including the point to be smoothed), with  $n$  being equal to, or greater than the order of the polynomial [38]. In addition, it can be shown that the same algorithm can be used to calculate processed first and second derivatives of the signal [39].

Mathematically, for the processing of a signal by using a 2nd order polynomial and 7 data points, this can be represented as;

$$y_t = \frac{(-2x_{t-3} + 3x_{t-2} + 6x_{t-1} + 7x_t + 3x_{t+2} - 2x_{t+3})}{21} \quad (3.5)$$

### 3.7 Building the Labview Testing Environment and User Interface

The labVIEW testing environment was designed to provide a visual representation of the data being fed into the sensor suite during operation. It was a considerable advantage to be able to visually study the data produced by the system in real time and highlights the benefits that labVIEW's graphical user interface provide to the end user.

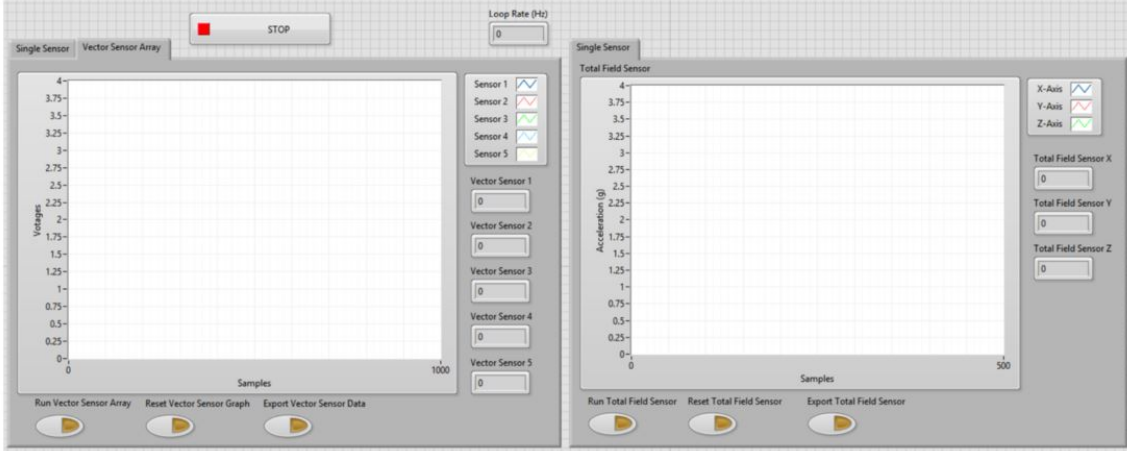


**Figure 3.14:** The graphical user interface that was built for the purpose of testing the system, while the implementation of this should not be used during the actual deployment of the sensor because of the load it would place on the myRIO, this interface was essential for testing purposes, and is identical to the 'bare-bones' program except no data is fed to the UI

# **Chapter 4**

## **Sensor Suite Development**

The following sections will attempt to outline the factors and considerations, as well as the various steps undertaken when simulating the conditions of a drone mounted sensor suite.

## 4.1 Operational Limitations of Fluxgate Magnetometers

### 4.1.1 Determination of Ideal Sensor Height

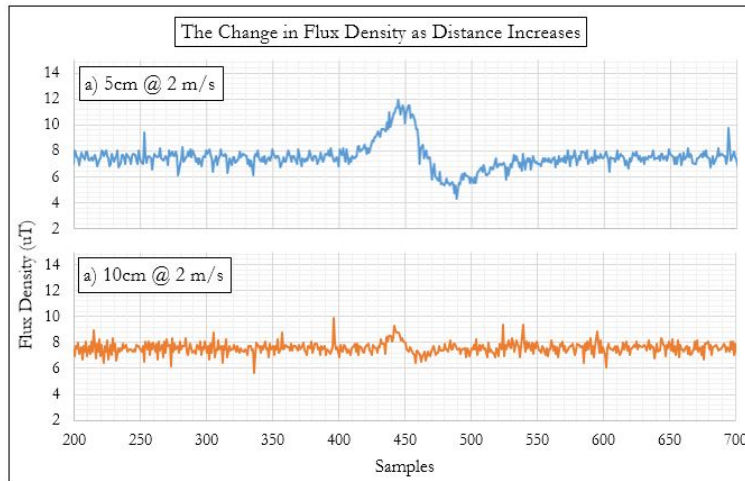
Prior to the initiation of this research project it was found that magnetic field density of a magnetic source falls off in accordance with the inverse cubed law due [40]. Thus it was already assumed that in order to determine the location of any ferrous materials the eventual sensor suite would need to be situated in close proximity to the target.

The inverse cubed law theoretically applies to all forces, which obey the inverse square law when applied to point entities. This can be represented for a Magnetic Force  $F_p$  through:

$$F_D \propto \frac{1}{R^3} \quad (4.1)$$

Where  $F_D$  is the Force Field, and  $R = \text{distance}$ .

Thus it was clear before testing commenced that in order to produce the clearest readings, it would be essential to have the sensors as close to the ground as possible. This was demonstrated by simple analysis which can be seen in *Figure 4.1* below;



huh? square  
and cube  
laws?

You could have  
measured the fall off  
in signal and seen if it  
actually fit a cube  
law...

**Figure 4.1:** Flux Density  $B$  as measured by a single FLC-100 sensor, the limiting factor of distance was a major concern that will need to be addressed

### 4.1.2 Determination of Ideal Flight Speeds

In order to determine the ideal flight speed that should be attempted when using the magnetometers, the process for relatively simple. The speed of the moving ground was ramped up to the necessary speed before the meteorite was placed on the bed, the resulting signal should theoretically represent the passing of a flying drone over a stationary meteorite.

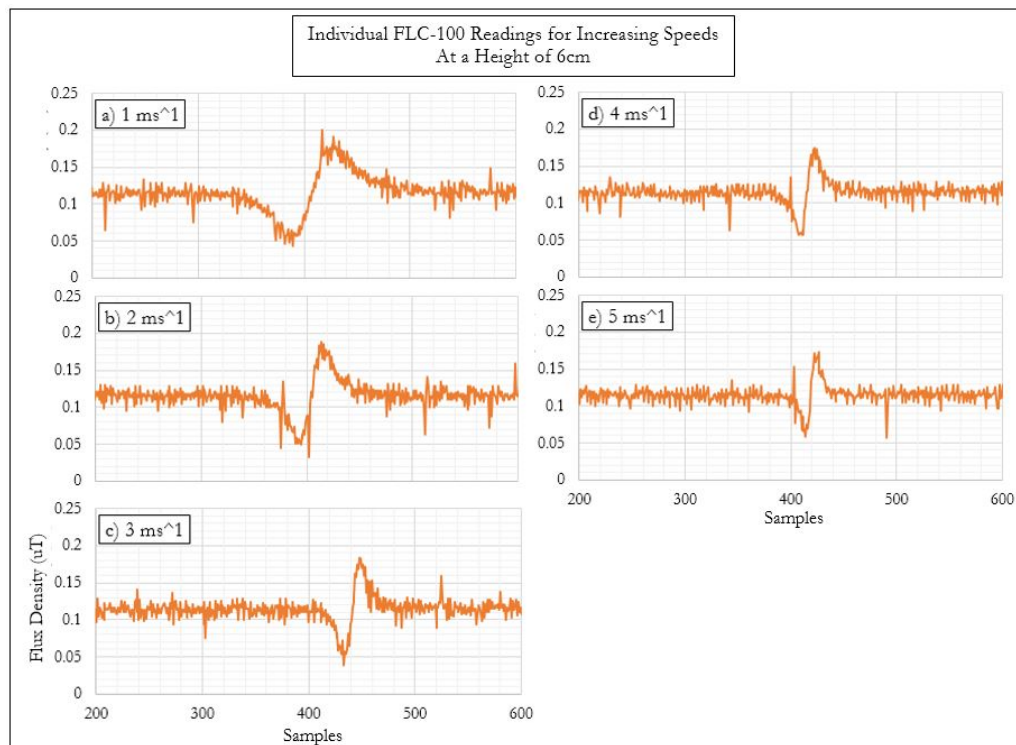


**Figure 4.2:** This figure displays the various in signal compression as speed increases. We also see a reduction in the height of the waveform which results in a signal height equal to that of a noise peak. This can be best seen in d) at  $5\text{ms}^{-1}$ .

for a meteorite of known depth (distance from boom), could you determine size from the area under the curve...

## 4.2 Sensor Suite Noise

### 4.2.1 Analogue Noise

From the testing of sensor accuracy (*See 4.2.3*) early on in the project it was found that when measuring the signal produced by the FLC sensors that noise would be a factor that would need to be addressed. This section will describe the problems that arise when analogue data is sampled for filtering in a digital system, in particular, the significant of aliasing. The various digital filters proposed in the Project Methodology will be attempted with their results documented.

### 4.2.2 Noise Considerations

In order to ensure maximum effectiveness, any eventual UAV mounted magnetic system needs to be able to collect high quality magnetic data which will allow for the detection and identification of meteorites on or near the surface of any terrestrial body.

Any measured signal will almost inevitably include some amount of noise or signal resulting from the surrounding environment that will need to be overcome. This could be from the electrical hardware that make up the system or, in the case of a UAV mounted system, the significant intrinsic magnetic noise that will be produced by the materials from which it is constructed, or from its various components.

As such it was determined that there are two possible ways that the noise signal can be minimised:

1. Through the implementation of software compensation or filtering
2. Through critical design considerations that look at the shielding or distancing of noise producing materials from the sensor suite

### 4.2.3 Establishing Sensor Accuracy and Resolution

A key parameter for establishing the accuracy of any magnetic sensor is a study of its output resolution. In a magnetic measurement system, resolution can be defined as the smallest increment of position change which can be detected and indicated by the output.

#### FLC-100

From the data sheets provided for the FLC-100, it can be seen that it featured an accuracy of  $\pm 2\%/\pm 0.3\mu T$  at  $20^\circ C$  with a bandwidth of 1kHz. In order to assess the performance of this sensor and ensure that it conforms to these limiting factors, the earth magnetic field in the lab was measured at 1kHz. Now it is understood that in order to achieve the best results, if you have a bandwidth  $f_b$  then under ideal conditions, the sampling rate should greater than  $2f_b$  in order collect all the information there is in that signal [41] [42]. However due to the limitations of the system when sampling from 8 analogue sensors and a TTL GPS while providing a graphical representation of the data 1kHz was a satisfactory achievement. These concerns will be addressed in later sections.

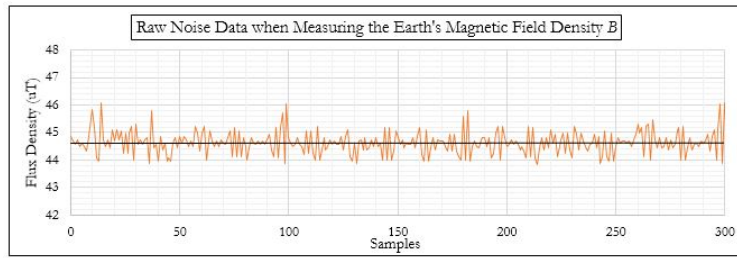


**Figure 4.3:** The accuracy of the FLC-100 when measuring the Earths Magnetic Field, in order to ensure that noise was kept to a minimum, experiment was conducted at 10pm with a shielded cable and the FLC-100 a minimum of 80cm for any external circuitry. A simple temperature sensor gave the room temperature at  $16^\circ C$

The Bin Range was plotted with a standard deviation  $0.39\mu T$ . This was sufficiently close enough to the provided data sheet and was deemed satisfactory

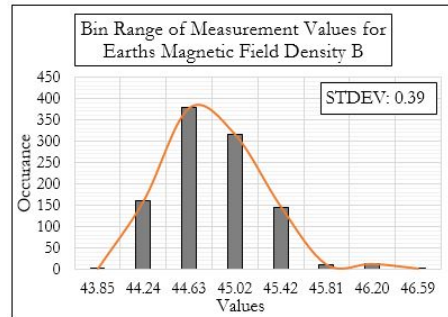


**Figure 4.4:** Bin Ranges of the variation when measuring the Earth's magnetic field

## FLC-370

The specifications of the FLC-370 list the accuracy at  $\pm 1\% / \pm 0.5 \mu T$  with a temperature of 20°C at a bandwidth of 1kHz.

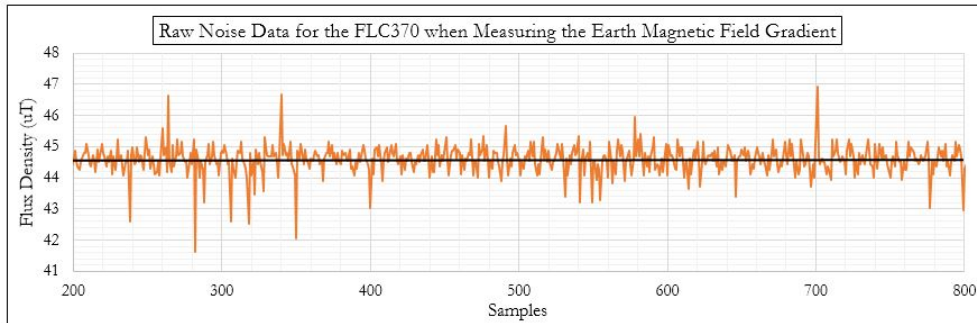


**Figure 4.5:** The accuracy of the FLC-370 when measuring the Earth's Magnetic Field with a Voltage input of 5V, the experiment was conducted at 9:30pm with a shielded cable and the FLC-370 a minimum of 80cm from any external circuitry. A simple temperature sensor gave the room temperature at 18°C

The standard deviation was calculated and the Bin Range plotted below with a standard deviation of  $0.44 \mu T$ . While this is slightly more than the FLC-100, this was still considered a satisfactory result. However it should be noted that this error is expected to increase if the input voltage is increased.

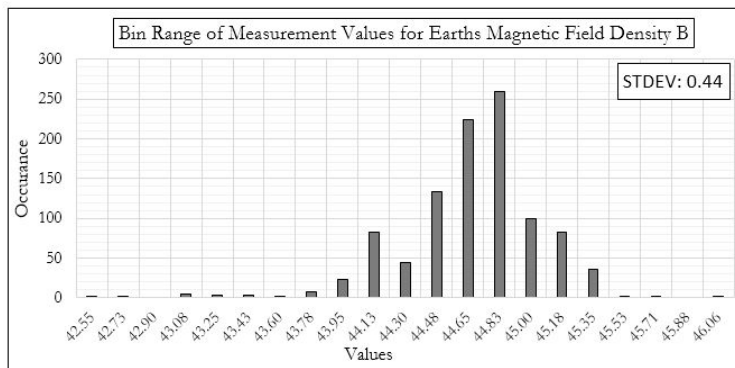


**Figure 4.6:** Bin Ranges of the variation when measuring the Earth's magnetic field

#### 4.2.4 Aliasing

While the electrical noise in a sensors output is due to small random changes in voltage potential and it is the primary factor limiting its measurement, noise was also seen to arise from the sampling of high frequency data at insufficient sampling rates. When data is sampled at discrete points in time, faster sampling periods increase the accuracy of identifying faster changes in the signal. From research conducted it was found that the with a sine wave of period  $P$  the signal should be sampled at a sampling rate of least twice the maximum frequency component of the signal of interest [42].

If the sampling rate is too low, aliasing will make the high frequencies appear as if they were lower frequencies [43] with no reduction in overall noise. This can best be described through *Figure 4.7* below where the signal in blue gives the illusion of a recurring noise signal when in reality it is a representation of interpolated values from the points in orange sampled at too low a rate.

good. Why not use  
the word Nyquist  
theorem or sampling  
rate or frequency

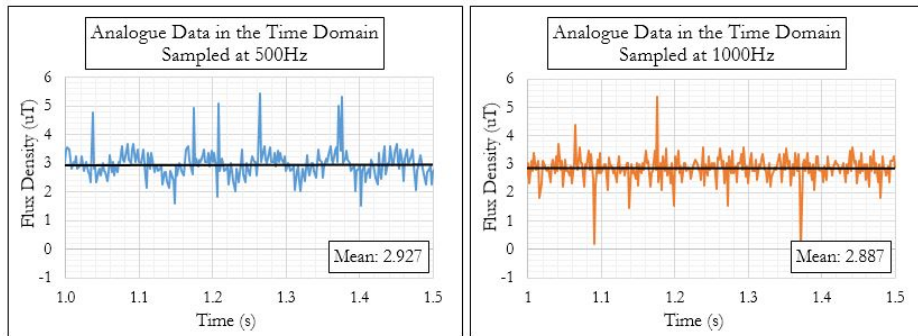


**Figure 4.7:** Here we can see the very real effects that aliasing has on data provided from the FLC-100 as the sampling rate is increased from 0.5kHz at half the bandwidth ( $1/2f_b$ ) to 1kHz (the sensor bandwidth  $f_b$ )

Additional tests were conducted in order to determine the appropriate sampling frequencies for various fractions of  $f_b$  however once it was found that the implementation of gradiometric setup would combat these issues they were no longer pursued.

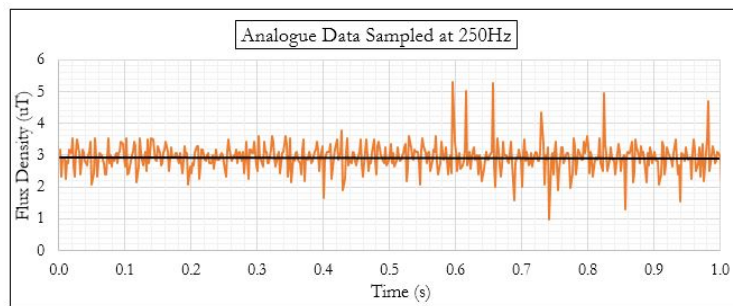


**Figure 4.8:** Visually there is no aliasing at a sampling frequency of 250Hz

## Fast Fourier Transform

The harmonic content is an illustration of the magnitude of a waveform versus the frequency. This is sometimes called the frequency spectrum and it allows for the visualisation of a waveform according to its frequency content [44].

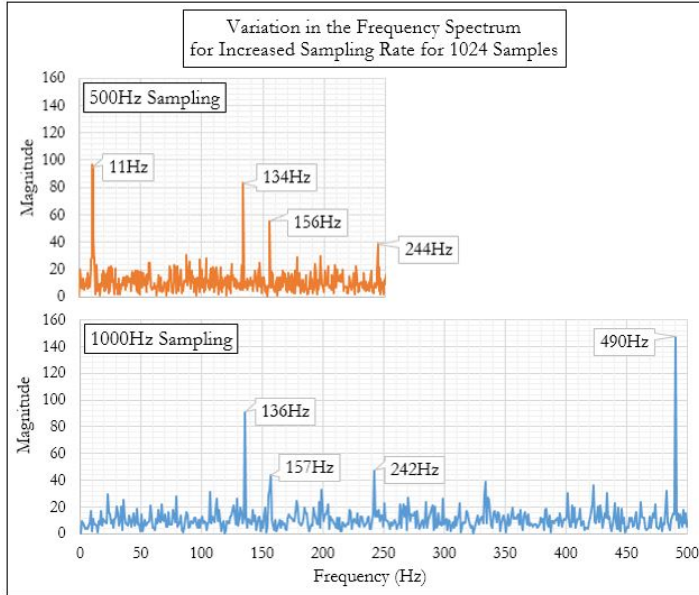


**Figure 4.9:** The two waveforms from Figure 4.7 plotted in the Frequency Domain, note the occurrence of an  $11\text{Hz}$  wave, this was assumed to be the result of the aliased waveform

Through these plots in the frequency spectrum we can see that there is a presence of background noise at various frequencies, these being  $\approx 135\text{Hz}$ ,  $\approx 156\text{Hz}$  and  $\approx 243\text{Hz}$ . However there is also a presence of a signal that occurs when the signal is sampled at  $500\text{Hz}$  of  $11\text{Hz}$ , and we can safely assume that this is the signal that is a result of the interpolated values from the points sampled at too low a rate. There is also the presence of a noise at the frequency of  $490\text{Hz}$  which cannot be explained.

There were additional experiments carried out to measure the background noise at different periods of the day at varying sampling rates however despite continued efforts there seemed to be no way to remove the presence of these background frequencies. Various attempts at shielding the sensor suite were conducted with the introduction of shielded cables and late night measurements when there was minimal external disturbances.

the descriptions of a,b and c should be in the figure caption as well.

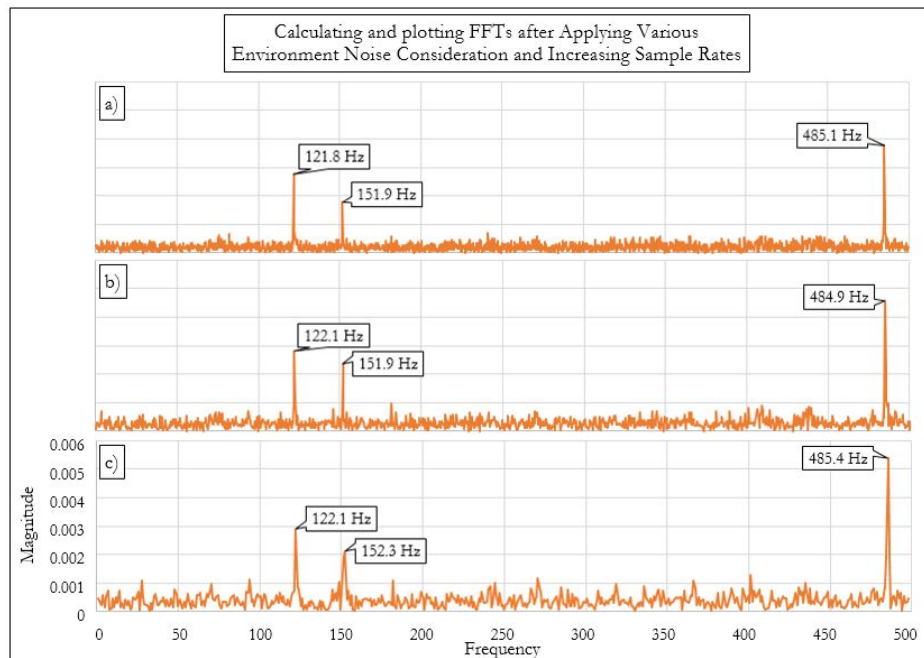


**Figure 4.10:** Three of a number of FFTs attempted to determine the frequency content of the noise signal.

These transforms feature sampling rates of  $1000\text{Hz}$  for *c*) with 1024 samples,  $2000\text{Hz}$  for *b*) with 2048 samples, and  $4000\text{Hz}$  for *b*) with 4096 samples over the same frequencies as before. In addition these transforms represent different attempts to manage the noise frequencies of the signal. With both *a*) and *c*) taken outside with the myRIO, away from any potential noise sources in the lab. It is important to note however that any frequency above  $1500\text{Hz}$  is not possible on the Teensy 3.2 and so these experiments were purely speculative in nature. No quantitative data could be determined as to the source of this background noise and so it was assumed that they form part of the inherent noise of the sensors.

#### 4.2.5 Digital Compensation for Analogue Noise

In section 3.6.1 of the Project Methodology, various potential digital filters were suggested and researched with the intention of eventual implementation into the sensor suite. The following section will attempt to outline the various filters attempted and their effectiveness at removing unwanted noise from signals.

## Comparison of Digital Filters for Noise Reduction

In the end there were really only two digital filters that were considered for implementation into the sensor suite, due to the demands of the system any microcontroller won't be able to complete complex processing without severely reducing the sampling rate of the suite. As such it was determined that any filter that would be implemented would need to be easy to apply and easy to modify, but most importantly, it needed to be a recursive function that could build on itself to drastically reduce computation time.

While this is not too much of an issue for the myRIO, it is most certainly a massive consideration for future implementation of the sensor suite as the myRIO is unfit for implementation on a drone. Thus two filters were chosen, these were the Savitzky-Golay 2nd order polynomial filter and the Moving Average first order polynomial filter. These two filters were implemented on the following signal in order to get a comparison of their function and noise reduction.

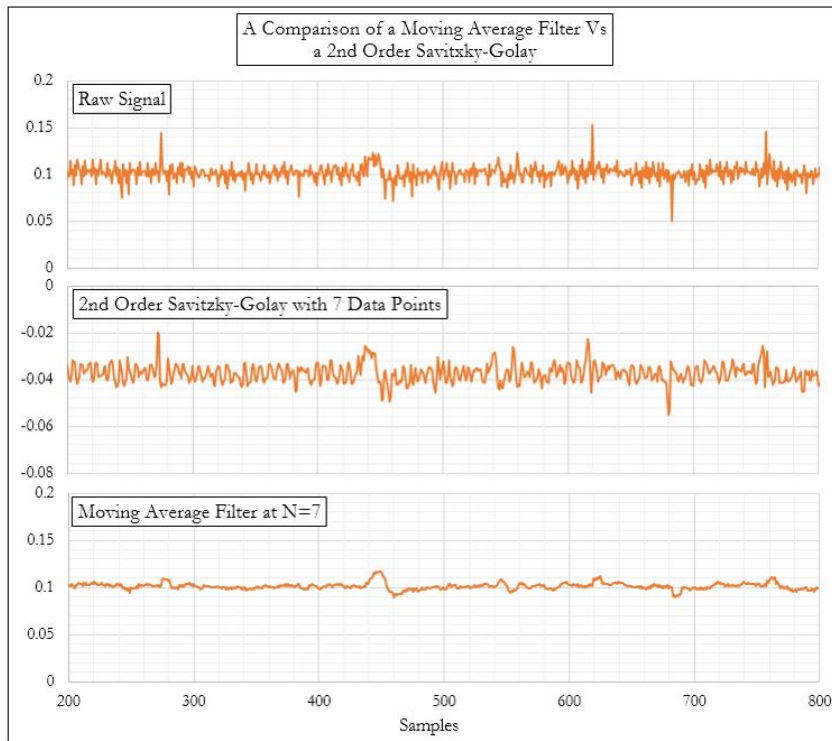


**Figure 4.11:** This figure attempts to illustrate the results of the various experiments conducted to determine the effectiveness of these filters on a digital signal. As can be seen, for a 7-point moving average roughly two thirds of the noise is removed and with a 7-point quadratic function only about half the noise is removed

Here it can clearly be seen that the moving average filter gives the best noise reduction for  $N=7$ . This was repeated for increasing values of points in order to determine the S/N Ratio reduction for increasing points on N.

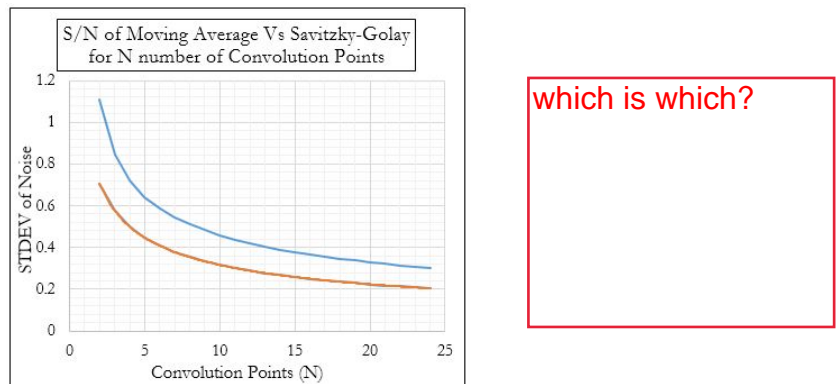


**Figure 4.12:** *The Effects of Moving Average Filters vs Savitzky-Golay for increasing values of N*

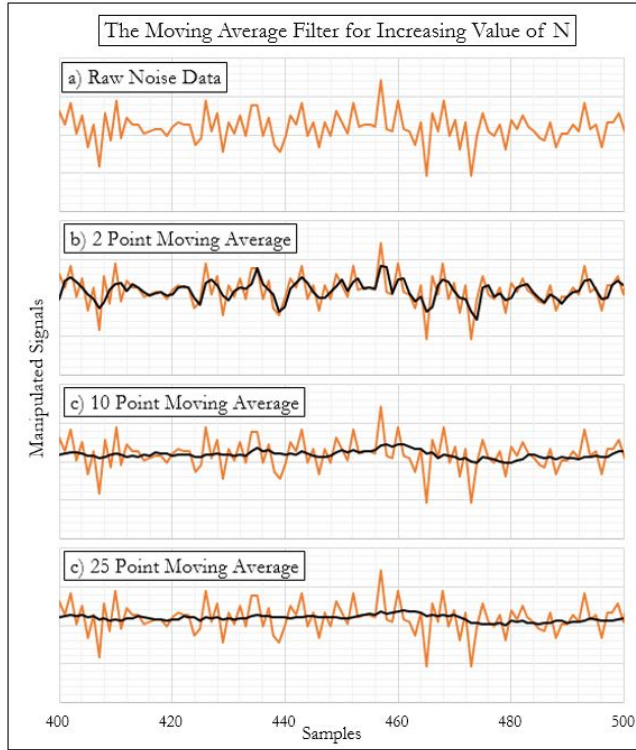
Again, it is clear that the Moving Average Filter is vastly superior to the Savitzky-Golay for any reasonable value of N. And while it can be assumed that they will approach each other as we increase N, this will only result in wasted computation time.

### Moving Average Filter for Noise Reduction

The following data demonstrates the time domain response of a Moving Average filter of filter length N implemented post sampling in Excel on the noise produced by the FLC-100. To maximise the significance of the findings, the produced output (black) has been plotted over the raw data (orange).

### Advantages of the Moving Average Filter

It can be seen that when implementing the moving average filter that the smoothing of the filter decreases the amplitude of random noise but reduces the sharpness of rises and falls of the signal. When plotting the S/N in Figure 4.14 it can be seen that the noise reduced can be quantified as the square root of the number of points in the average. i.e. Ideally, a moving average filter for  $N = 100$  will reduce the noise by a factor of 10.



I wonder how median and mode filters would perform.. These are also computationally easy, but are not affected by random high noise data points.

**Figure 4.13:** This signal is filtered with increasing values of points  $N$ . As the number of points increases the noise becomes significantly less defined, this can be seen in the S/N plot of the same data following, see Figure 4.14, however it is important to note that the edges also become less sharp. This may prove to be an issue for the sharp pulses that are produced when measuring a magnetic field at increased speeds

### 4.3 Gradiometric Implementation of Fluxgate Magnetometers on the Sensor Suite

As was explored in **INSERT** of the Literature Review, there are numerous advantages to the implementation of using a fluxgate gradiometer array as opposed to measuring independent fluxgate sensors. Reiterating what was explored previously, the magnetic gradient is measured by calculating the difference in flux density over the distance between the sensors, mathematically represented as;

$$G = \frac{B_1 - B_2}{\Delta d} \quad (4.2)$$

or in the case of measuring across multiple sensors

$$G = \frac{\Delta B}{\Delta d} \quad (4.3)$$

Looking at this equation it can be seen that there is a fairly simple mathematical

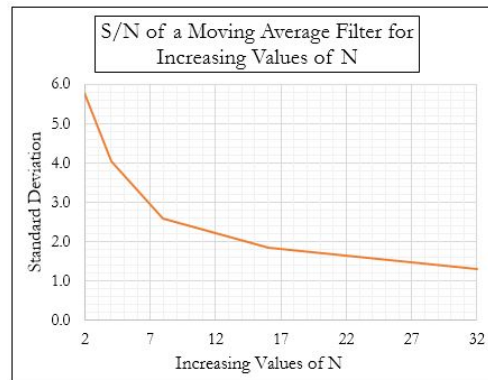


**Figure 4.14:** The Signal to Noise (S/N) ratio for increasing values of  $N$  for the noise data shown in Figure 4.13

relationship for any constant  $\Delta B$ . Ideally, the sensitivity of  $G$  should increase as the distance increases with a exponential reduction in the S/N ration, producing;

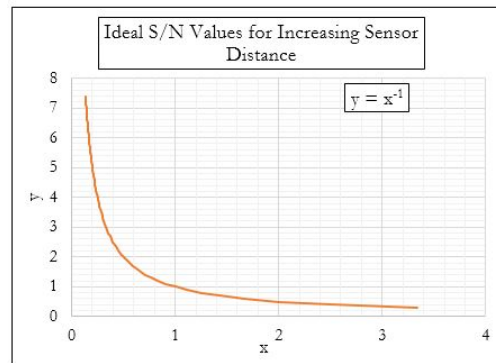


**Figure 4.15:** A representation of the ideal S/N ratio for increasing distances

Immediately the conclusion can be that the further the sensors are placed apart the higher the higher the accuracy of the sensor suite. However due to the sensitivity of the sensors there are obvious limitations to this as can be seen when studying the effects of a gradiometer set-up to increase resolution.

The noise levels of a magnetic gradient setup was then conducted with increasing values of  $\Delta d$  which can be seen in Figure 4.16. While there was some minor variation as can be expected from any analogue sensor, it conformed to the expected result. Thus it was determined that ideally, the sensors should be placed as far apart as reasonably possible in order to obtain the highest possible sensitivity.

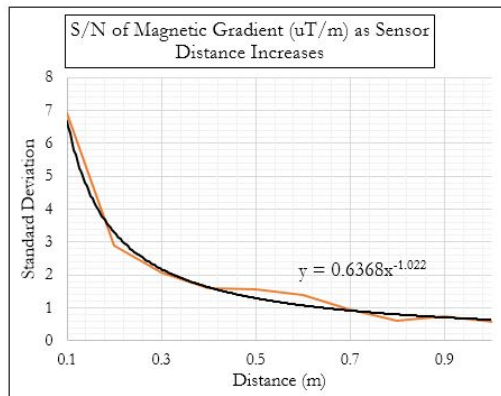
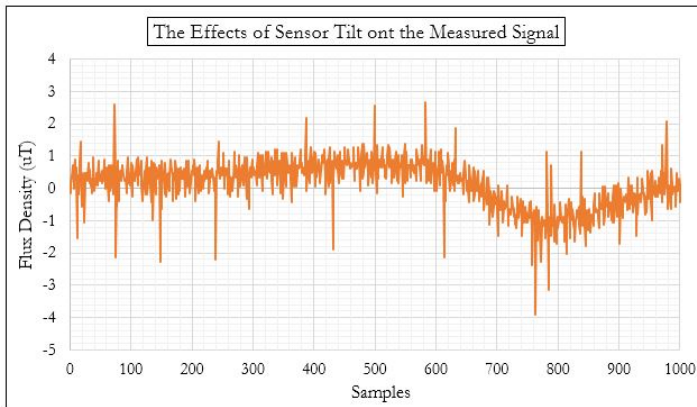


**Figure 4.16:** A representation of the ideal S/N ratio for increasing distances

### 4.3.1 Sensor Orientation and Tilt

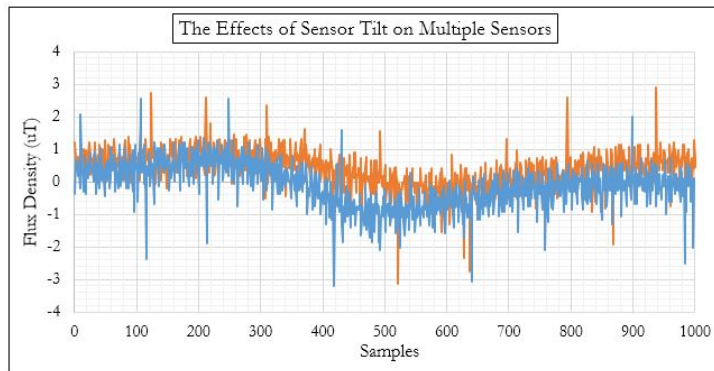
Magnetometer measures the components of earth's magnetic field through the voltage induced by a change in flux density on the coil of the sensor. As the sensor is fixed on the Printed Circuit Board (PCB) the readings will change according to the orientation of the sensor itself. A such it is paramount that the sensor maintains a fixed position during operation.

Figure 4.17 represents the issues that arise from sensor tilt during operation, the FLC-100 being sampled was tilted upwards by  $\approx 15^\circ$ , the resulting change is flux density produces a signal that is similar to that of a potential meteorite.



**Figure 4.17:** The flux density signal produced after the sensor was subjected to a tilt in the z direction

This has profound issues in the event of magnetometer tilt and presents a serious limitation in the application of this technology on any drone system as it would be constantly affected by pitch and yaw. The next step was to determine the affect this would have on a total system of two or more sensors. Figure 4.18 illustrates the changes that affect two fluxgate sensors that are subjected to a pitch of  $\approx 15^\circ$ , spaced 30cm apart.



**Figure 4.18:** The flux density signal produced after the sensor was subjected to a tilt in the  $z$  direction

The change in flux mirrors the previous figure and highlights the potential consequences of attaching individual magnetometers to a moving system. However the implementation of the Magnetic Gradient of these two measurements done provide a significant amount of stability to the signal.

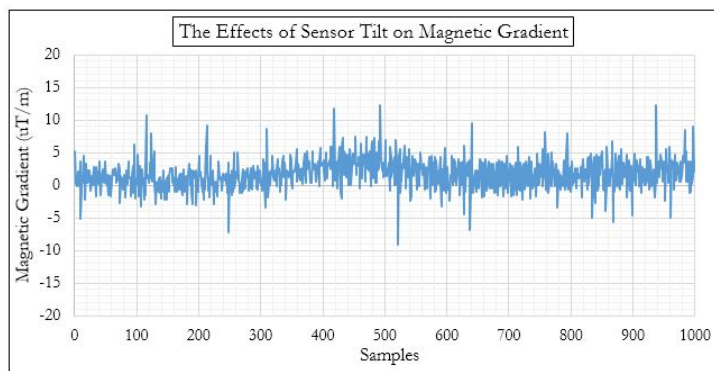


**Figure 4.19:** Here we can see that Magnetic Gradient is significantly more stable when the entire system is subjected to the same change in orientation

However this does not translate across to the tilt of a single sensor in either the  $x,y$  or  $z$  direction as all produce a change in magnetic flux that is not shared by their partner. *Figure 4.20* highlights the issues that arise when one sensor is subjected to change in orientation, while this may seem like an unlikely occurrence due to the fact that all sensors will be fixed to the boom of the sensor suite, this data was produced from two sensors fixed with their coils in parallel before the sudden tilt of the sensor suite. Sensor 2 (blue) height was reduced from 30cm above the medium to 5cm and then back while Sensor 1 (Orange) was left mostly stationary. The effect is parallel to that of a potential magnetic field source.

This is only exacerbated when implemented in a gradiometer set-up;

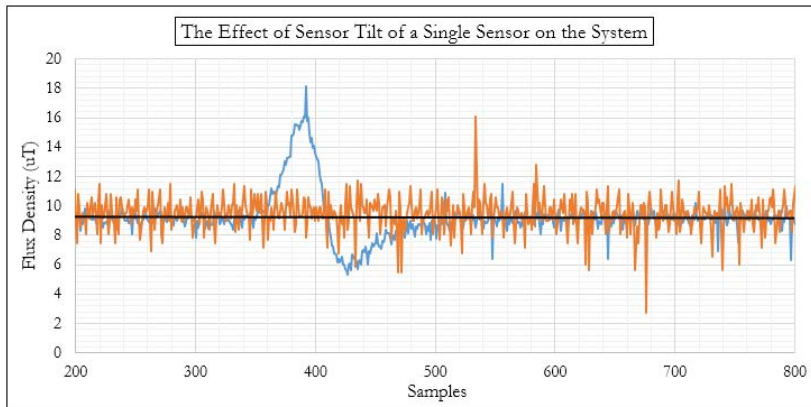


**Figure 4.20:** Here that the rabid movement of a single sensor up and down will significantly screw the results produced

a little more exact language would be good. Also, these figure captions are inadequate. Always give a legend showing that the two colours represent

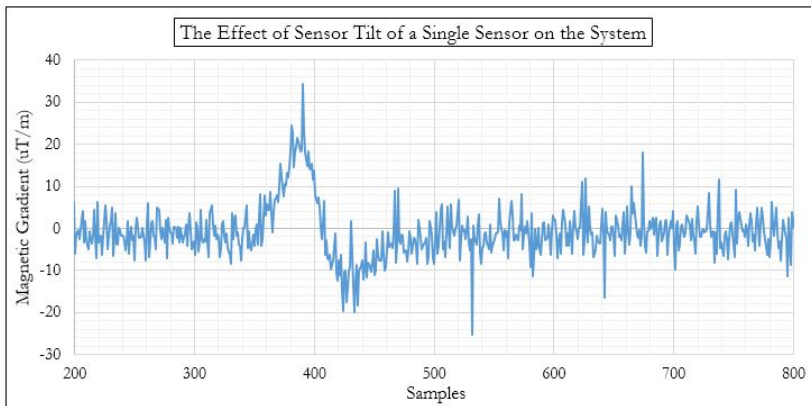


**Figure 4.21:** The stability of the Magnetic Gradient is almost non-existent

The benefit of a Magnetic Gradient is its ability to notice subtle changes in flux density between measurement points and thus is unable to deal with these un-uniform orientation changes across the measurement sources.

This is an important section, but I am not convinced you have solved the problem presented by changing sensor angles.

### 4.3.2 Influence on Aliasing

Immediately the benefits of using a gradiometric or differential sensor set-up can be seen in *Figure 4.22* below when two FLC-100s are sampled at half their bandwidth, which is known to cause significant aliasing issues.

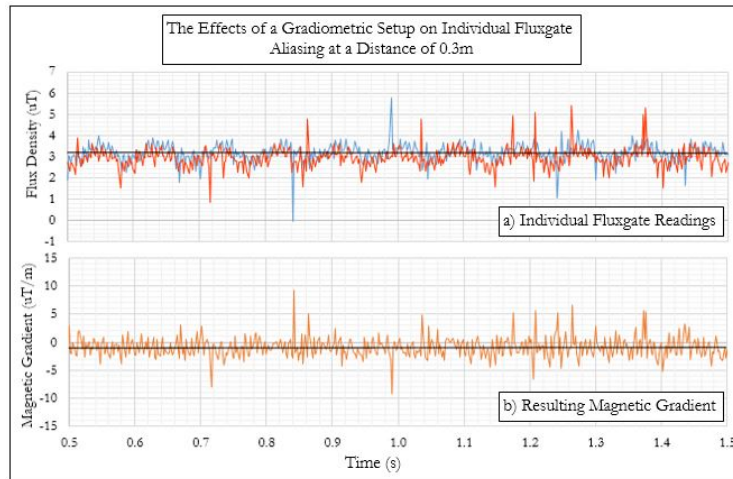


**Figure 4.22:** The magnetic gradient calculated at a sensor distance of 0.3m. Due to the signal monitoring, processing and storage that will be required from any microcontroller that is utilised in this research project, the proposed system is estimated to sample at a lower rate than 2kHz and as a result, aliasing is a concern. This can be addressed however through the use of a gradiometric design which helps negate the effects, and while not entirely successful, is critical prior to digital filter implementation as will be seen below

Due to the sampling rate, aliasing is clearly being seen by both sensors, this is instantly counteracted when employed in a gradiometric set-up.

OK good.

### 4.3.3 Individual Fluxgate Sensors Vs Magnetic Gradient

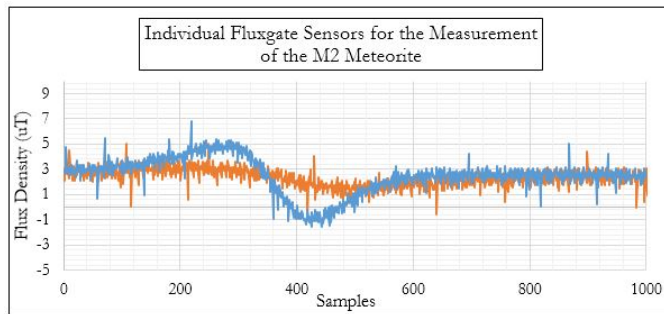


**Figure 4.23:** test

Figure 4.24 shows the differential effect of the readings obtained from the individual fluxgate readings depicted in Figure 4.23. The sensors were spaced at a distance of 0.3m apart at a height of 0.8m above the moving ground. The M2 meteorite was depicted as travelling at a speed of  $1ms^{-1}$  offset at a horizontal distance of 0.1m from Sensor 1 (Blue) and therefore 0.2m away from Sensor 2 (Orange). Somewhat surprisingly the presence of the meteorite can be seen across both sensors, however it is clearly more defined for Sensor 1.

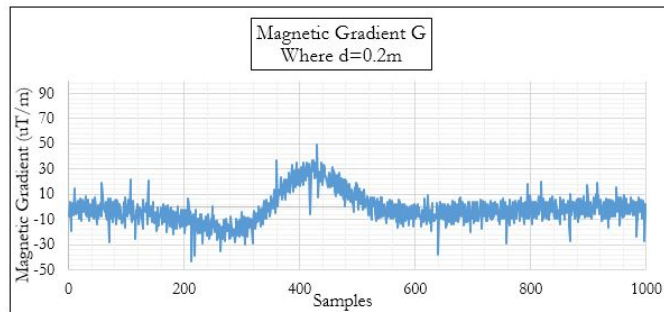


**Figure 4.24:** The result of the magnetic gradient of 4.23, the signal is relatively well defined but the minute measurement of the meteorite of Sensor 2 reduced the effectiveness of the data

## Speed

As can be seen from the previous section, in order to properly assess the effectiveness that a gradiometric setup will have on the sensor suites ability to detect meteorites at increasing speeds, the sensors needed to far enough apart that there was sufficient baseline to give the best possible results. It was found that at a distance of more than 15cm from the M2 that the likelihood of detection is low and at distances approaching 30cm, detection is impossible. Thus in order to test the effect of speed on magnetic gradient signal compression it was decided that the control sensor would be more than 20cm away from the meteorite measuring the ambient magnetic field of the surrounding area. What we received was a crisp set of data that also further highlighted the increase in sensitivity that arises as distance between the sensors increases.

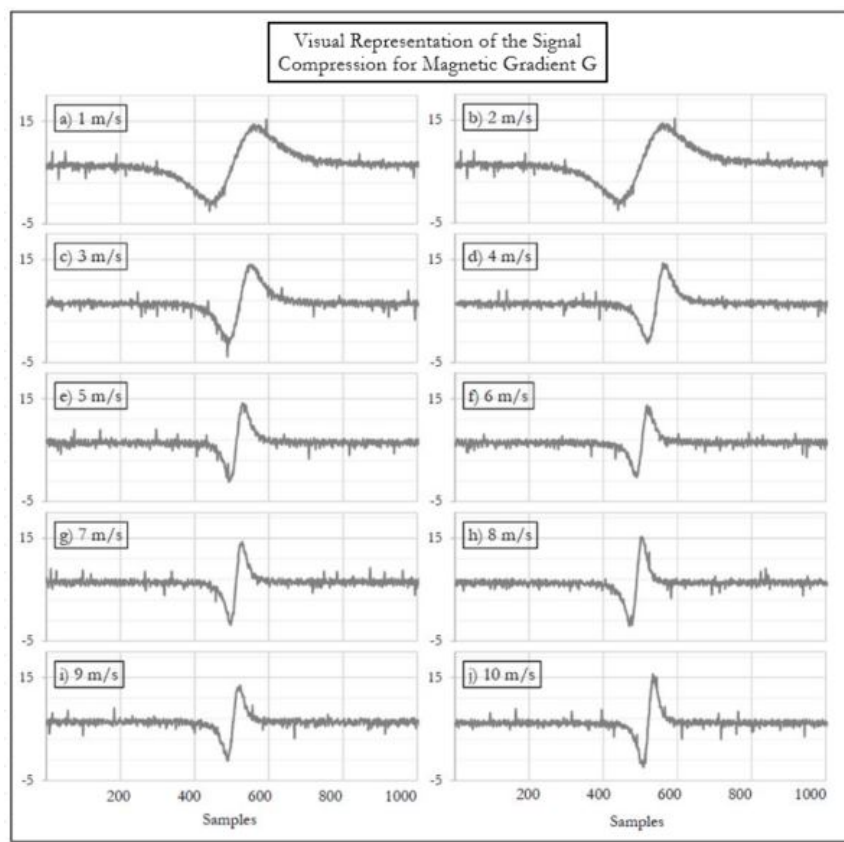


**Figure 4.25:** The effect that an increase in speed has on the compression of the measurement signal. Note that noise is reduced when compared to the similar experiment conductor in Section 4.2. Both experiments were conducted at a height of 6cm at the same location of testing at a sampling rate of 1000Hz

While the noise levels at  $5\text{ms}^{-1}$  were at the same level as the signal for individual FLC-100 readings, when employed as in a gradiometric set-up we can potentially double the speed that can be achieved by a drone system.

#### 4.3.4 Prevalence of Noise in a Gradiometric Sensor

Unfortunately, it seems that noise is still significant issue when looking for the presence of meteorites, due to their relatively low magnetic field density it is almost impossible to detect a meteorite from a height above 8cm. In Figure ?? we can see that due to the prevalence of noise in the system, even with a gradiometric set-up in place, this is significant issues with discerning the M2 meteorite without the use of a moving average filter.

missing  
labels are  
quite  
common.

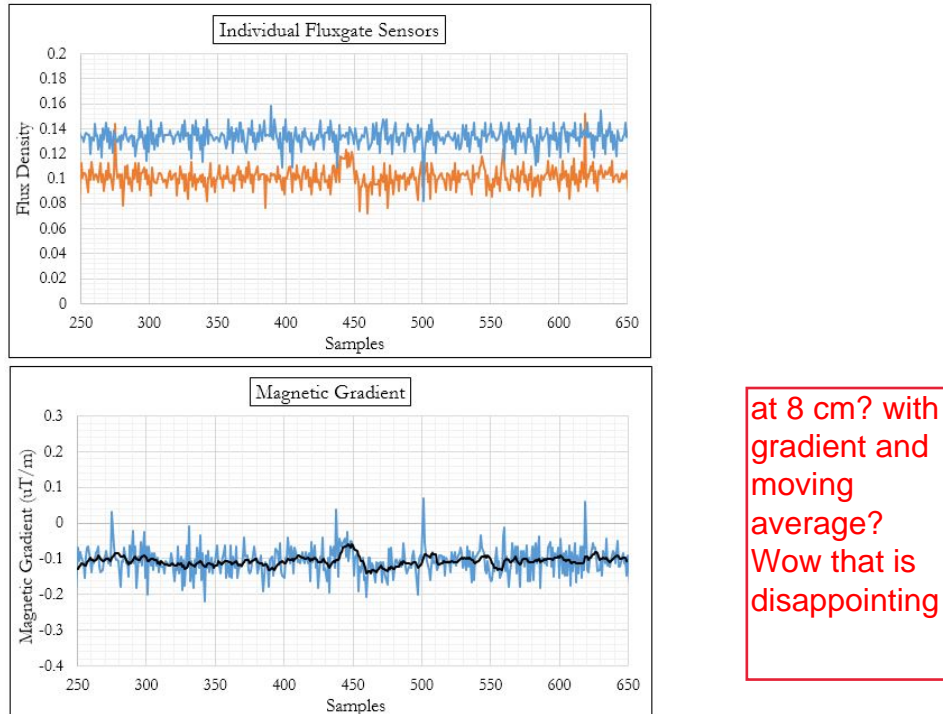


**Figure 4.26:** Test

However once a moving average filter of  $N=10$ , is applied the presence of the meteorite is discernible.

## 4.4 Initial Design Prototyping

Once detailed testing had been conducted, the final design and technical specifications for the sensor suite were decided with the final product being developed through a detailed design process.

### 4.4.1 CAD

The 3D design of the system was critical in identifying design flaws and pinpointing serious build problems, and the construction of 3D printed prototypes was an essential tool for rapidly making cost efficient design modifications.

The data collected from this initial prototype testing can then be used to change the prototype models and improve the product or design for future revisions of the project.

### 4.4.2 Materials and Parts List

#### Hardware

The Sensor Suite will contain

- 4x FLC-100 Single Axis Fluxgate Magnetometers
- 1x FLC-370 Triaxial Fluxgate Magnetometers
- 1x LS20031 GPS Receiver

#### Structure

It was decided that ABS plastic would be optimum choice for the sensor suite, as it features numerous benefits:

- Strength
- Moderate detail level
- Rigid
- Resolution size of 0.25mm

## 4.5 Final Prototype

### 4.5.1 Sensor Orientation and Layout

The Triaxial FLC370 is to be mounted in the centre of the sensor suite, this is partly due to its high sensitivity but the primary reason is that the three components will be invaluable in later field test of the sensor suite. This is because the use of a three component fluxgate will help to eliminate the need to precise orientation and will help to provide the much needed data regarding local field lines. It will also store the magnetic field in the x and y directions which may prove critical to later data analysis. This will be critical should the sensor suite be deployed on a slope. The FLC-100s are to be mounted horizontally from the FLC-370 and care will be taken to ensure that they are in parallel.

The distance between the sensors was eventually decided on as 25cm as this provided a good resolution while still maintaining the ability to sense a potential meteorite. There will be an attempt to ensure that the sensor wiring have a certain amount of give so that the sensor can be moved  $\pm 5\text{cm}$  left or right of the original mounting. This is to ensure that there is the option to increase or decrease sensitivity depending on the situation.

### 4.5.2 Sensor Suite CAD

The final prototype was designed using 3D CAD software and was estimated to weight a total of  $\approx 350\text{g}$ , with a total length of 1050mm from either end. Every sensor would feature a cover for protection in the event of a crash while ensuring that the solution was kept as light as possible. In order to achieve this, the resolution of the 3D printed parts was kept at 15% with a hexagon structure filling the interior of each part for strength.

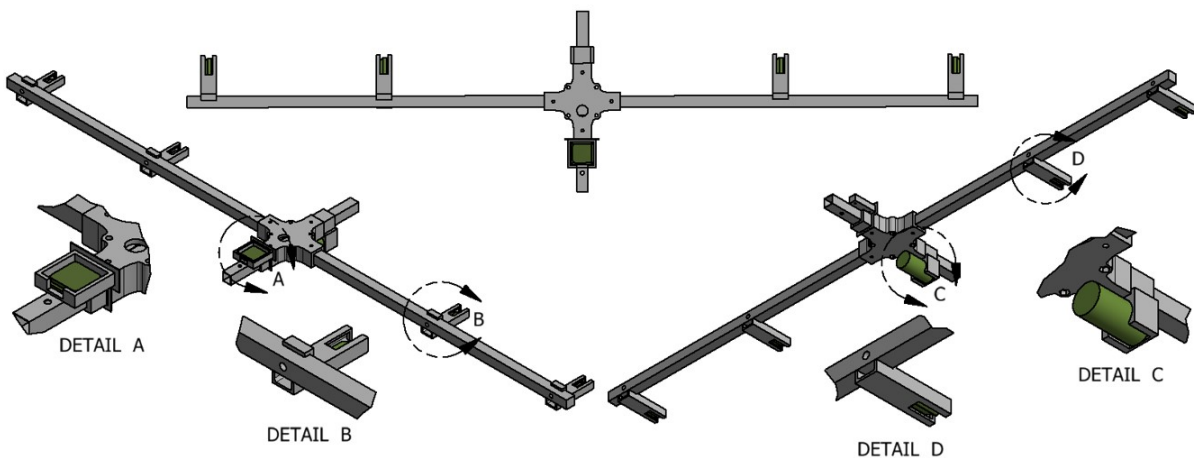


**Figure 4.27:** The Final Sensor Suite CAD Model Before Construction Commenced

Additional detailed designs can be found in Appendix C

## 4.6 Production

The sensor suite was constructed as per the design requirements listed above.

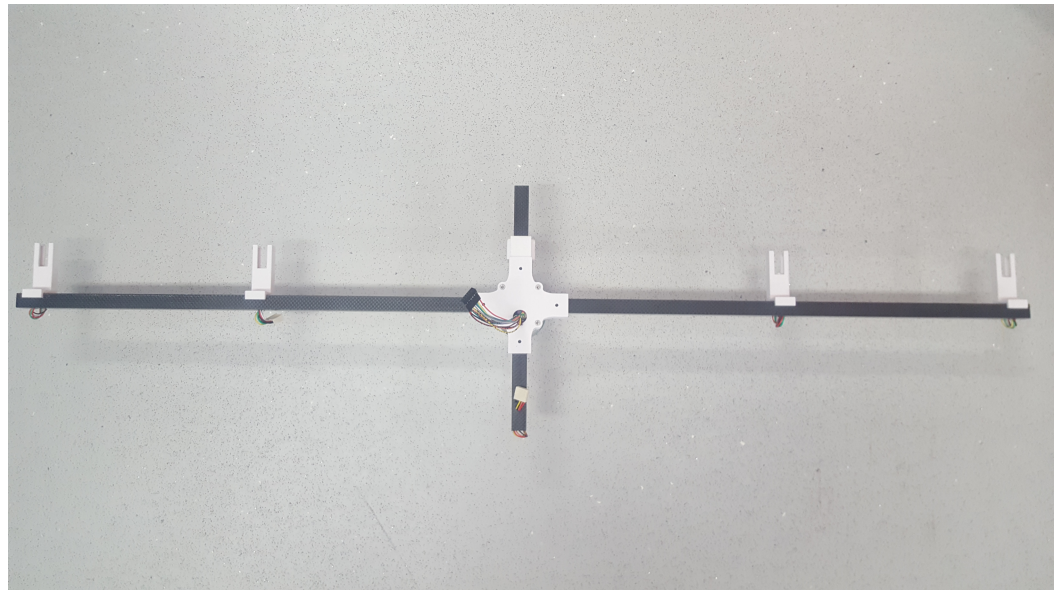


**Figure 4.28:** *The Completed Sensor Suite*



**Figure 4.29:** Sensor Suite can also be attached to a pole to ease of carrying, this will enable for the eventual field testing in the event that a drone cannot be sources

## 4.7 Data Imported for the Sensor Suite

The data is exported to a USB, either through the myRIO or the teensy, however it is important to note that should the teensy be desired there will be a requirement for the purchase of a USB shield as the GPS unit is already communicating via a TTL to USB circuit. The data exported by the myRIO can be seen through [Figure ??](#) and saved to either a USB or host computer as a .csv file, enabling for it to be opened in various types of data processing programs, including MATLAB, EXCEL and Notepad.

#### 4.7 Data Imported for the Sensor Suite

	A	B	C	D	E	F	G	H	I	J	K	L	M	N	O	P
1	Samples - X-Axis FLC100z-1 (B)	FLC100z-2 (B)	FLC370z (B)	FLC100z-3 (B)	FLC100z-4 (B)	FLC370v (B)	FLC370v (B)	Filtering	G 1	G 2	G 3	G 4	Latitude	Longitude	Valid	
2	1	0.09517	0.10615	0.11714	0.10615	0.11592	5.42967	41.3208	No	0.04392	0.03925	0.03925	-0.03908	0.00	0.00	
3	2	0.09883	0.10981	0.11226	0.12446	0.10737	5.36864	41.1987	No	0.04392	0.00875	-0.04357	0.06835	0.00	0.00	
4	3	0.0915	0.09883	0.10005	0.11836	0.11714	5.42967	41.4429	No	0.02932	0.004357	-0.05539	0.00488	0.00	0.00	
5	4	0.10249	0.10371	0.10493	0.09395	0.09395	5.70589	40.7715	No	0.00488	0.004357	0.039214	0	0.00	0.00	
6	5	0.08296	0.10249	0.09395	0.12568	0.10737	5.06346	41.0155	No	0.07812	-0.0305	-0.11332	0.07324	0.00	0.00	
7	6	0.10859	0.10737	0.11226	0.10615	0.10127	5.55174	41.1377	No	0.00488	0.017464	0.021821	0.01952	0.00	0.00	
8	7	0.10127	0.08174	0.10249	0.12202	0.10493	5.3076	40.6494	No	-0.07812	0.074107	-0.06975	0.06836	0.00	0.00	
9	8	0.10005	0.10127	0.10859	0.11592	0.09915	5.73485	41.3208	No	0.00488	0.026143	-0.026178	0.09768	0.00	0.00	
10	9	0.09761	0.07808	0.08418	0.11958	0.11348	5.36864	41.9311	No	0.07812	0.021786	-0.12643	0.02444	0.00	0.00	
11	10	0.10371	0.10127	0.1147	0.1269	0.10615	3.96483	41.4429	No	-0.00976	0.047964	-0.04357	0.083	0.00	0.00	
12	11	0.09272	0.10493	0.10371	0.11958	0.10371	5.36864	41.4429	No	0.04884	-0.00436	-0.05668	0.06348	0.00	0.00	
13	12	0.10371	0.09272	0.10615	0.12202	0.10249	5.61278	41.1377	No	-0.04396	0.047964	-0.05668	0.07812	0.00	0.00	
14	13	0.09028	0.11592	0.10493	0.11714	0.09883	5.97899	41.0766	No	0.10256	-0.03925	-0.04361	0.07324	0.00	0.00	
15	14	0.14399	0.10981	0.0915	0.11836	0.10615	4.94139	40.3442	No	-0.13672	-0.06539	-0.09593	0.04884	0.00	0.00	
16	15	0.10249	0.10127	0.11103	0.1147	0.10493	4.27001	41.748	No	-0.00488	0.034857	-0.01311	0.03908	0.00	0.00	
17	16	0.09761	0.1147	0.10005	0.12202	0.10249	5.3076	41.9922	No	0.06836	-0.05232	-0.07846	0.07812	0.00	0.00	
18	17	0.09883	0.09517	0.10737	0.1208	0.09639	5.61278	41.748	No	-0.01464	0.043571	-0.04796	0.09764	0.00	0.00	
19	18	0.09883	0.10981	0.08418	0.1147	0.10859	5.67381	41.5039	No	0.04392	-0.09154	-0.109	0.02444	0.00	0.00	
20	19	0.10493	0.10371	0.1147	0.05854	0.10493	5.18553	41.5649	No	-0.00488	0.03925	0.0200571	-0.18556	0.00	0.00	
21	20	0.10493	0.10493	0.10371	0.1147	0.10493	4.88036	41.8091	No	0	-0.00436	-0.03925	0.03908	0.00	0.00	
22	21	0.10371	0.10127	0.09517	0.14888	0.15132	5.91796	40.4053	No	-0.00976	-0.02179	-0.19182	-0.00976	0.00	0.00	
23	22	0.08418	0.09761	0.10249	0.1208	0.10005	5.55174	41.4429	No	0.05372	0.017429	-0.06539	0.083	0.00	0.00	
24	23	0.0915	0.10981	0.09517	0.12812	0.10371	5.49071	41.2597	No	0.07324	-0.05229	-0.11768	0.09764	0.00	0.00	
25	24	0.09517	0.10371	0.10859	0.10005	0.10127	5.24657	41.8701	No	0.03416	0.017429	0.0305	-0.00488	0.00	0.00	
26	25	0.11226	0.10615	0.05244	0.11836	0.1147	5.67381	41.687	No	-0.02444	-0.19182	-0.23543	0.01464	0.00	0.00	
27	26	0.09761	0.10005	0.10859	0.1269	0.09639	5.3076	41.5039	No	0.00976	0.0305	-0.06539	0.12204	0.00	0.00	
28	27	0.1147	0.10859	0.09028	0.10493	0.10615	5.24657	41.1987	No	-0.02444	-0.06539	-0.05232	-0.00488	0.00	0.00	
29	28	0.0945	0.11727	0.11147	0.11726	0.11720	5.17464	41.746	No	0.06248	0.04883	0.04883	0.00	0.00	0.00	

what about time?  
Why no time?

**Figure 4.30:** An example of the data exported by the sensor suite, the layout is identical whether it comes from the myRIO or the Teensy

Bummer that you were not able to get data and try to process it.

# Chapter 5

## Conclusion and Outlook

In this thesis I have investigated the feasibility of using a magnetic gradiometer sensor suite to be fitted to an Unmanned Aerial Vehicle in order to perform low altitude magnetic measurements for meteorite detection. The proposed approach would allow for a considerable increase in geographic coverage and reduction in human resources as well as giving significant productivity and cost gains over conventional airborne surveys. Drones are incredibly well suited for many areas of terrestrial exploration, they can be mobilized and launched with minimal effort and require only a small team to operate and maintain. This work has clear relevance in an incredibly diverse range of search applications, such as the discovery of unexploded ordnance (UXOs), archaeological or geological sites, mineral deposits and planetary exploration

A key component of this project was the design and construction of a magnetic sensor suite for deployment on a drone platform. A testing system was developed to analyse and interpret this data to determine the location of any objects of interest. The collection of magnetic data on various meteorites and terrestrial rocks was performed with combined magnetic sensors in laboratory and field tests. The findings of this research project indicate that the use of magnetic sensing is a somewhat appropriate way to detect meteorites at low altitudes from a moving unmanned aerial vehicle. However because the detection quality is principally limited by sensor accuracy, the application of more sensitive magnetometers would be recommended to increase sensor precision as opposed to the additional manipulation of the digital data to increase detection distance.

Noise was a considerable issue throughout this research project, due to the low magnetic fields emanating from the meteorites, however the use of two sensors in a gradiometric layout has been found to minimise the effects of noise somewhat, however it is important to note that spikes in the data translate across to the gradiometric data and can significantly skew results. Thus it is essential to ensure that the sensors are fixed in place and very precisely aligned before deployment. This is essential because once the sensors are out of equilibrium with each other we can see massive spikes in the magnetic gradient indicating the sharp change in the magnetic flux. While this can be somewhat compensated for, the magnetic gradient will still feature a rise which could give the illusion of a potential item of interest. In addition there should be the implementation

of a feedback system from another analogue sensor such as an accelerometer as this will give an indication to the pitch, yaw, and roll of the system and calculations can be made accordingly.

An investigation into the feasibility of using on-board filtering was performed and it was found that despite its simplicity, the moving average filter is optimal for reducing signal noise while retaining a sharp step response. In addition, due to its recursive nature the moving average filter requires almost no computation time when compared to the other digital filters available and as such can be deployed on any potential Microcontroller for real-time data processing. Thus through the implementation of this filter, the sensor suite was configured to mitigate noise from the electrical components of any potential drone system however the magnetic sensing suite will require additional refinement to correctly support its use on an aerial vehicle. This will include the adaptation of filter equations and code to account for the noise attributed to the vehicles components and ensuring that an appropriate level of robustness and durability is implemented for use in remote areas or hard environment conditions. The integration of a GPS into the sensor suite verifies that a potential drone system could locate and log meteorite locations in real time. However due to the manner of implementation the timing requirements of serial connectivity impaired the sampling rate of any Microcontroller that was storing the data. Sample rates were considerably lowered due to the issues with communications with the GPS Unit, unfortunately the wait time required by the GPS between serial connections required a few ms ending in a sampling rate of  $\approx 250\text{-}300\text{Hz}$ . Thus it has been determined that the GPS should store data separately to the Microcontroller through a client system.

In conclusion, the findings of this report indicate that while the desired application of the technology is possible, there are severe limitations regarding the operational constraints of such a system. Limited by height, it is highly unlikely that an autonomous drone will be able to maintain a constant altitude. In addition, the spacing of the sensors presented a considerable limitation, reducing the footprint of the suite to just over one metre. And while it is known that an increased distance improves sensitivity, the likelihood that both sensors could pass over a potential meteorite increases exponentially as the sensors are spaced further apart. As such it is recommended that for the applications of this research project, that the sensors are spaced no more than 30cm away from each other as this will provide a solid compromise between sensitivity and accuracy. Lastly, one of the fundamental assumptions of this research project was that the implementation of a low flying drone would be vastly superior to a ground based drone however the limitations of this technology indicate that mounting the sensor suite on a drone will produce disagreeable results and dramatically increase noise levels, and as such further work will be conducted into the possibility of deployment on a wheeled or tracked robot as this would dramatically reduce the chances of rapid un-uniform changes in elevation and tilt of the sensor suite.



# Appendix A

## Sensor Test-Bed Code

### A.1 Teensy 3.2 Testing Code

```
void setup()  {
    Serial.begin(38400);
}

void loop()  {
    delay(500);

    float magGrad;
    float sensorDist = 0.25;

    int sensorA0 = analogRead(0);
    int sensorA1 = analogRead(1);
    int ref = 2.5;

    String A0String = "A0: ";
    String A1String = "A1: ";

    float A0Voltage = sensorA0 * (5.0 / 1023.0);
    float A0uTesla = (A0Voltage-ref)*50;

    float A1Voltage = sensorA0 * (5.0 / 1023.0);
    float A1uTesla = (A1Voltage-ref)*50;

    magGrad = ((A0uTesla - A1uTesla)/sensorDist);

    Serial.println(A0String + A0Voltage);
    Serial.print(" V");
    Serial.println(A1String + A1Voltage);
    Serial.print(" V");
    Serial.println(" ");
    Serial.println(A0String + A0uTesla);
    Serial.print(" uT");
    Serial.println(A1String + A1uTesla);
    Serial.print(" uT");
    Serial.println(" ");
    Serial.println("Magnetic Gradient: ");
    Serial.print(magGrad);
    Serial.print(" uT/m");
}

}
```

# **Appendix B**

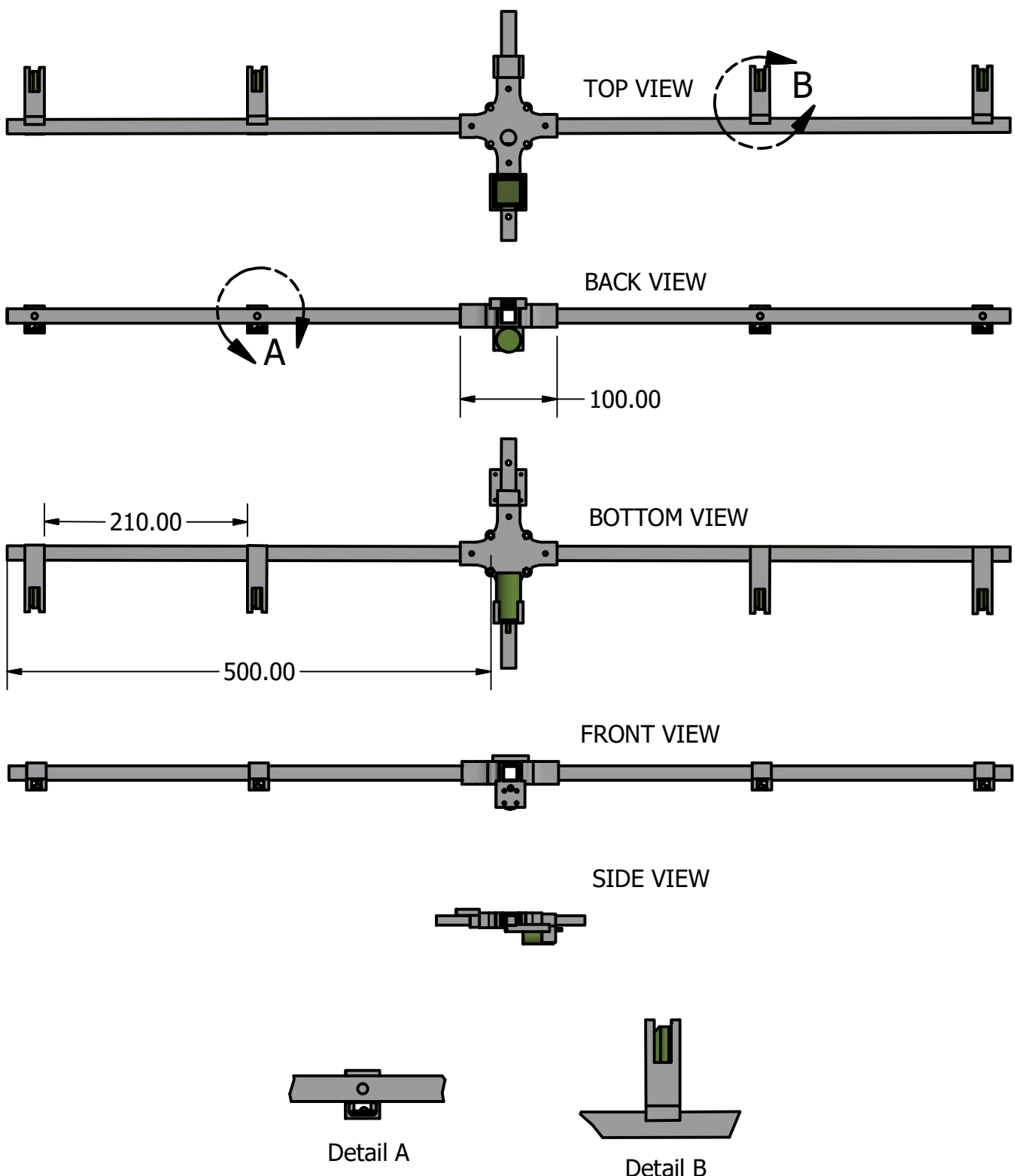
## **Final Design Documents**

### **B.1 Detailed Sensor Suite Designs**

Appendix

C

1.1

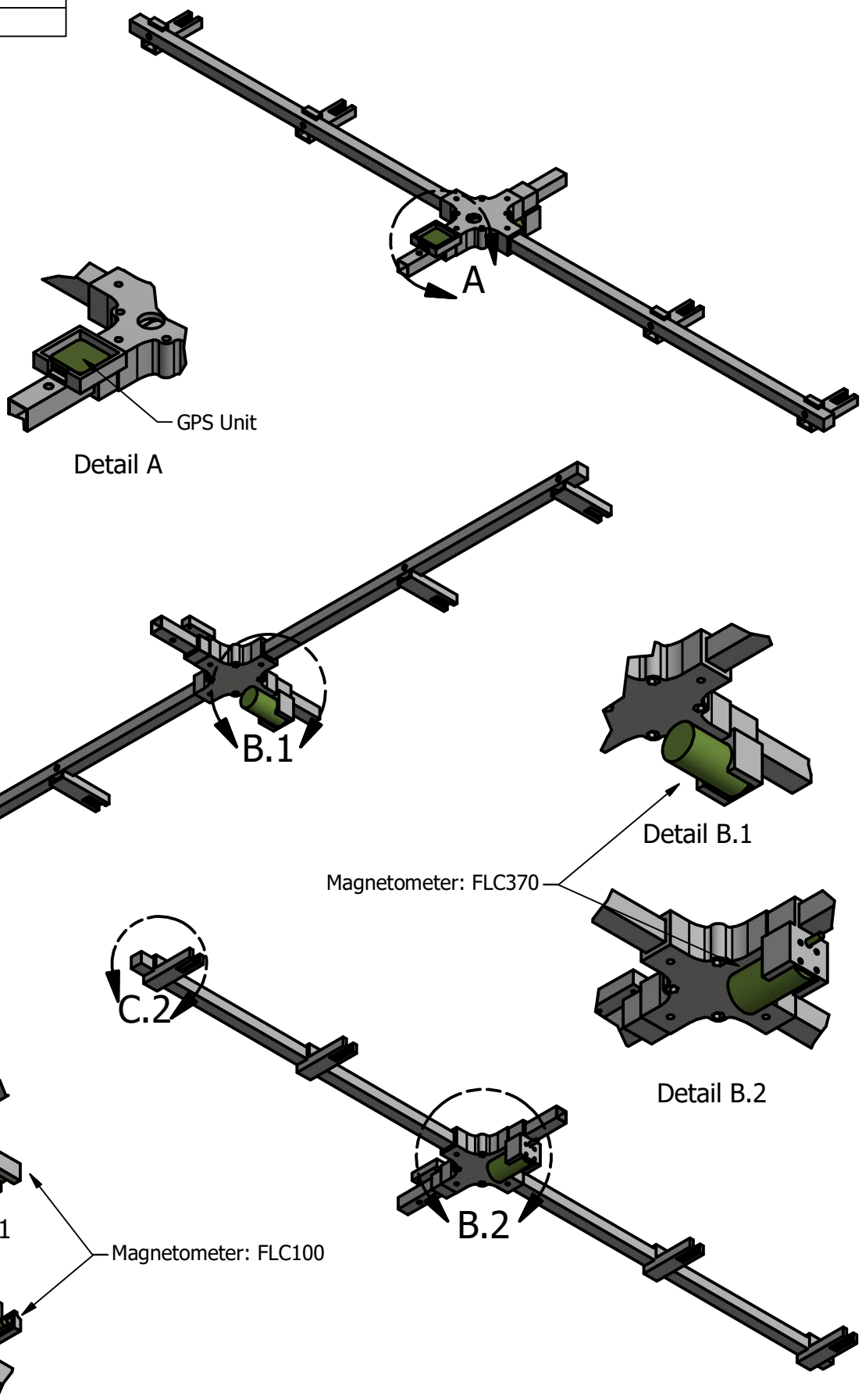


REVISION HISTORY		
REV	DESCRIPTION	AUTHOR
161110 A	Complete Sensor Suite	Adrian Orellana

Appendix

C

1.2



REVISION HISTORY		
REV	DESCRIPTION	AUTHOR
161110 B	Complete Sensor Suite	Adrian Orellana



# References

- [1] R. Harvey, The Origin and Significance of Antarctic Meteorites, *Chemie der Erde - Geochemistry*, vol. 63, no. 2, p. 93147, 2003.
- [2] ElkShoulder, . J. Franklin, O. Yawea, K. Gchachu, J. Simmons, B. A. Cohen and H. E. Newsom, Meteorite Identification And Classification Using Magnetic Susceptibility, *Lunar and Planetary Science XXXVII* , 2006.
- [3] Liam Pedersen, Robotic Deployment of Electro-Magnetic Sensors for Meteorite Search, in Proceedings of the 1998 IEEE International Conference of Robotics & Automation, Leuven, Belgium, May, 1998.
- [4] D. Moorhouse, Hyper-spectral Imaging for Airborne Meteorite Detection, 29 October 2014.
- [5] C. C. Mardon and A. A. Mardon, The Use of Side-Looking Airborne Radar in the Discovery of Meteorites in the Antarctic, *Lunar Exploration Analysis Group*, Alberta, Canada, 2015.
- [6] D. S. Apostolopoulos, L. Pedersen, B. N. Shamah, K. Shillcutt, M. D. Wagner and W. L. Whittaker, Robotic Antarctic Meteorite Search: Outcomes, in *IEEE International Conference on Robotics & Automation*, Seoul, Korea, 2001.
- [7] A. Foessel, D. Apostolopoulos and W. Whittaker, Radar sensor for an autonomous antarctic explorer, *Robotics Institute, Carnegie Mellon University*, Pittsburgh.
- [8] A. Martin and C. Martin, The use of Geographic Remote Sensing, Mapping and Aerial Photography to Aid in the Recovery of Blue Ice Surficial Meteorites in Antarctica, *Edmonton, Canada: Golden Meteorite Press*, 2009.
- [9] A. W. R. Bevan, Meteorites recovered from Australia, *Journal of the Royal Society of Western Australia*, , vol. 9, pp. 33-42, 1996.
- [10] K. Wells, The Australian desert the outback of Australia, 23 August 2013. [On-

- line]. Available: <http://www.australia.gov.au/about-australia/australian-story/austn-desert-outback>. [Accessed 6 April 2016].
- [11] A. Bevan, Australian Meteorites, R.O. Chalmers, Commemorative Papers (Mineralogy, Meteoritics, Geology), vol. Records of the Australian Museum Supplement 15, pp. 1-28, 1992.
- [12] M. Marquardt, Down to Earth With: Antarctic meteorite hunters, Earth Magazine, 15 December 2012. [Online]. Available: <http://www.earthmagazine.org/article/down-earth-antarctic-meteorite-hunters>.
- [13] S. A. Macintyre, Magnetic Field Measurement, CRC Press LLC, 1999.
- [14] T. S. Murali, What is the physical difference between magnetic flux density (B) and magnetic field strength (H)?, Quora, June 2016. [Online]. Available: <https://www.quora.com/What-is-the-physical-difference-between-magnetic-flux-density-B-and-magnetic-field-strength-H>.
- [15] ELSTER LLC, Magnetic Field Gradient Defined, 2001. [Online]. Available: <http://mriquestions.com/what-is-a-gradient.html>.
- [16] T. Bratland, R. Schneider, C. H. Smith and M. J. Caruso, A New Perspective on Magnetic Field Sensing, Honeywell Inc, 1998.
- [17] J. E. Lenz, A Review of Magnetic Sensors, Proceedings of the IEEE, vol. 78, no. 6, pp. 973-989, 1990.
- [18] D. Faber, Feasibility of instrumental detection of meteorites in Antarctica, Gateway Antarctica, Canterbury, 2011.
- [19] G.E.M Systems Advanced Magnetometers, Advantages of Magnetic Gradiometers, 2016. [Online]. Available: [http://www.gemsys.ca/pdf/Advantages\\_of\\_Magnetic\\_Gradiometers.pdf?lbisphreq=1](http://www.gemsys.ca/pdf/Advantages_of_Magnetic_Gradiometers.pdf?lbisphreq=1).
- [20] N. O. Mariita, The Magnetic Method, in Short Course II on Surface Exploration for Geothermal Resources, Naivasha, 2007.
- [21] P. W. Schmidt and D. A. Clark, The Magnetic Gradient Tensor: Its Properties and Uses in Source Characterization, The Leading Edge, vol. 25, pp. 75-78, 2006.
- [22] T. McConnell and B. Dragoset, Introduction to this Special Section: Magnetic gradiometry, The Leading Edge, vol. 25, p. 45, 2006.

- [23] D. Tilley, Ground Magnetic Surveys Seeing Beneath The Rocks, GEOLOGY for Investors, [Online]. Available: <http://www.geologyforinvestors.com/ground-magnetic-surveys-seeing-beneath-the-rocks/>.
- [24] Analog Devices, Inc. Edited by Walt Kester, Section 6: Digital Filters, in Mixed-Signals and DSP Design Techniques, Newnes, 2003, pp. 6.1-6.39.
- [25] S. W. Smith, The Scientist and Engineer's Guide to Digital Signal Processing, California Technical Publications, 1997.
- [26] PJRC, Teensy USB Development Board, PJRC, 2016. [Online]. Available: <https://www.pjrc.com/teensy/>.
- [27] National Instruments, From Student to Engineer: Preparing Future Innovators With the NI LabVIEW RIO Architecture, National Instruments, 01 April 2014. [Online]. Available: <http://www.ni.com/white-paper/52093/en/>.
- [28] Stefan Mayer Instruments, Magnetic Field Sensor FLC 100, Dinslaken: Stefan Mayer Instruments.
- [29] Stefan Mayer Instruments, Magnetic Field Sensor FLC3-70, Dinslaken: Stefan Mayer Instruments.
- [30] Iowegian International Corporation, FIR Filter FAQ, 2015. [Online]. Available: <http://dspguru.com/dsp/faqs/fir>.
- [31] Arduino/Genuino, Arduino: Frequently Asked Questions, Arduino, 2016 . [Online]. Available: <https://www.arduino.cc/en/Main/FAQ>.
- [32] National Instruments, What Is LabVIEW?, 16 August 2013. [Online]. Available: <http://www.ni.com/newsletter/51141/en/>.
- [33] OANDA, Types of Moving Averages, 2015. [Online]. Available: <https://www.oanda.com/forex-trading/learn/technical-analysis-for-traders/moving-averages/types-of-ma>.
- [34] J. Devcic, Weighted Moving Averages: The Basics, Investopedia, 2016. [Online]. Available: <http://www.investopedia.com/articles/technical/060401.asp>.
- [35] J. F. Kenney and E. S. Keeping, Moving Averages, in Mathematics of Statistics, Princeton, Van Nostrand, 1962, pp. 221-223.
- [36] Weisstein, Eric W, Boxcar Function, From MathWorld—A Wolfram Web Resource,

- [Online]. Available: <http://mathworld.wolfram.com/BoxcarFunction.html>.
- [37] H. Lohninger, Savitzky-Golay Filter, in Teach Me Data Analysis, New York,, Springer-Verlag, 1999.
- [38] MathWorks, Inc., Filtering and Smoothing Data, MathWorks, Inc., [Online]. Available: <http://au.mathworks.com/help/curvefit/smoothing-data.html?requestedDomain=au.mathworks.com>.
- [39] J. Krumm, Savitzky-Golay Filters for 2D Images, Redmond: Microsoft Research, Microsoft Corporation, 2001.
- [40] X. Borg, The Inverse Cubed Law For Dipoles, The General Science Journal.
- [41] M. Kretschmar, Understanding Sensor Resolution Specifications and Effects on Performance, Machine Design, St. Paul, 2009.
- [42] T. Wescott, Sampling: What Nyquist Didn't Say, and What to, Wescott Seminars, 2016.
- [43] Chapter 2. Signal Processing and Modulation, [Online]. Available: <http://www.acfr.usyd.edu.au/pdfs/tr>
- [44] L. Klingenberg, Frequency Domain Using Excel, School of Engineering, San Francisco State University, San Francisco, 2005.
- [45] G. Bartington and C. E. Chapman, A High-Stability Fluxgate Magnetic Gradiometer For Shallow Geophysical Survey Applications, Archaeological Prospection, vol. 11, no. 1, pp. 19-34, 2004.
- [46] LOCOSYS Technology Inc., Datasheet of GPS smart antenna module, LS20030 3, New Taipei City: LOCOSYS Technology Inc., 2006.